

1                   ***Resilience in a time of stress: revealing the molecular***  
2                   ***underpinnings of coral survival following thermal bleaching events***

3  
4                   Brook L. Nunn<sup>1</sup>, Tanya Brown<sup>2,4</sup>, Emma Timmins-Schiffman<sup>1</sup>, Miranda Mudge<sup>1</sup>, Michael Riffle<sup>1</sup>,  
5                   Jeremy B. Axworthy<sup>2</sup>, Jenna Dilwort<sup>3</sup>, Carly Kenkel<sup>3</sup>, Jesse Zaneveld<sup>4</sup>, Lisa J. Rodrigues<sup>5</sup>,  
6                   Jacqueline L. Padilla-Gamiño<sup>2</sup>

7                   <sup>1</sup>Department of Genome Sciences, University of Washington, Seattle, WA, United States

8                   <sup>2</sup>School of Aquatic and Fishery Sciences, University of Washington, Seattle, WA, United States

9                   <sup>3</sup>Department of Biological Sciences, University of Southern California, Los Angeles, CA, United States

10                   <sup>4</sup>School of Science, Technology, Engineering & Mathematics, University of Washington, Bothell, WA,  
11                   United States

12                   <sup>5</sup>Department of Geography and the Environment, Villanova University, Villanova, PA, United States

14  
15                   \* **Correspondence:**

16                   Brook L. Nunn  
17                   brookh@uw.edu

18  
19                   Keywords: Coral bleaching, eco-physiology, proteomics, metabolic pathways, lipids,  
20                   microbiome, symbiont, urea

23 **Abstract**

24 Coral bleaching events from thermal stress are increasing globally in duration,  
25 frequency, and intensity. Bleaching occurs when a coral's algal symbionts are expelled,  
26 resulting in a loss of color. Some coral colonies survive bleaching, reacquire their symbionts and  
27 recover. In this study, we experimentally bleached *Montipora capitata* colonies to examine  
28 molecular and physiological signatures of intrinsic differences between corals that recover  
29 (resilient) compared to those that die (susceptible). All colonies were collected from the same  
30 bay and monitored for eight months post-bleaching to identify specific colonies exhibiting long-  
31 term resilience and survival. Using an integrated systems-biology approach that included  
32 quantitative mass spectrometry-based proteomics, 16S rRNA of the microbiome, total lipids,  
33 symbiont density and diversity, we explored molecular-level mechanisms of tolerance in pre-  
34 and post-bleached colonies and found biomarkers of resilience that can confidently identify  
35 resilient and susceptible corals before thermal-induced bleaching events. Prior to thermal  
36 stress, resilient corals were characterized by a more diverse microbiome and increased  
37 abundances of proteins involved in multiple carbon and nitrogen acquisition strategies, symbiont  
38 retention and acquisition, and pathogen resistance. Susceptible corals had early signs of  
39 symbiont rejection and had resorted to utilizing urea uptake pathways for carbon and nitrogen.  
40 Further, molecular signatures identified prior to bleaching were amplified after bleaching,  
41 suggesting these pathways may be deterministic in a colony's fate. Our results have important  
42 implications for the future of reefs, revealing molecular factors necessary for survival through  
43 thermally-induced bleaching events and providing diagnostic biomarkers for coral reef  
44 management.

45

46 **Significance statement**

47 Corals are being negatively impacted by the increase in the number and duration of thermal-  
48 induced bleaching events. There are, however, some individuals within a single species that will  
49 bleach and, after time, reacquire symbionts and physiologically recover while neighboring  
50 colonies will die. Here, we used a multidisciplinary approach to understand the biochemical  
51 details of the physiological changes of resilient and susceptible *Montipora capitata* to thermal-  
52 induced bleaching. Resilient corals were characterized by their use of multiple carbon and  
53 nitrogen acquisition strategies, metabolically active symbiont relationships, abundant antiviral  
54 proteins, and a diverse microbiome. We reveal a multi-factor molecular-level approach for  
55 confidently identifying resilient and susceptible coral colonies so that environmental managers  
56 can rapidly select quality candidates for propagation while in the field.

57

58

## 59 Introduction

60 Coral reefs are one of the most diverse and structurally complex ecosystems on Earth,  
61 providing shelter and habitat for many organisms (1). Tens of millions of people in more than one  
62 hundred countries have coastlines adjacent to coral reefs and depend on them for their livelihoods  
63 (2). Unfortunately, coral reefs are declining rapidly throughout the world due to pollution, coastal  
64 development, overexploitation (3, 4), and effects associated with climate change (5, 6). As global  
65 seawater surface temperatures increase, large-scale thermal-induced coral bleaching events  
66 (loss of distinctive coral coloration due to expelling of algal symbionts) are becoming  
67 increasingly common worldwide (7-9).

68 When water temperatures surpass a thermal threshold for a given coral species it leads to a  
69 breakdown in the association between the coral host and the symbiotic algae, Symbiodiniaceae.  
70 This breakdown results in symbiont expulsion and is termed “coral bleaching” due to the loss of  
71 the pigmented symbiont (3). In addition to the distinct colors, Symbiodiniaceae provide much of  
72 the energetic requirements for the host in the form of organic carbon and nitrogen  
73 photosynthetic byproducts (10). The expulsion of Symbiodiniaceae during bleaching events  
74 metabolically compromises the host (11), leading to reduced physiological performance,  
75 reduced reproductive capacity and can lead to widespread mortality.

76 A coral colony is a holobiont – a collection of organisms that includes the coral, its symbionts,  
77 and the microbial microbiome that exists on and in coral tissue. The diversity of the microbiome  
78 on corals frequently decreases with thermal-induced bleaching (12, 13). While some of these  
79 changes may be associated with the loss of Symbiodiniaceae, other changes in microbiome  
80 diversity appear to be driven by thermal stress directly (14). If cascading microbiome changes  
81 induced by bleaching disrupt relationships with bacteria or archaea that benefit coral host  
82 metabolism or pathogen defense, then those microbiome changes may also contribute to post-  
83 bleaching coral mortality.

84 Coral microbiomes demonstrate host specificity, bolstering the hypothesis that bleaching-  
85 induced microbiome disruptions play a significant role in host mortality (15-19). However,  
86 disentangling relationships between corals and their microbiomes is challenging without  
87 gnotobiotic models. Moreover, although genomic evidence and correlations between taxonomic  
88 abundance and disease provide some hints, it is still unclear which specific microbiome  
89 changes associated with bleaching or other stressors are helpful or harmful for the survival of  
90 the coral host. Indeed, while a rich literature documents alterations to microbiome structure and  
91 stability by many specific stressors and coral diseases — including changes to beta-diversity  
92 (20, 21), richness (22), and the abundance of particular taxa — far fewer data are available on  
93 which of these diverse microbiome changes best predict the future survival of coral hosts. Thus,  
94 data linking microbiome change with subsequent coral survival could be vital to interpreting the  
95 ecological consequences of shifts in bleaching-induced microbiome structure for corals.

96 Coral death due to the interconnected physiological and microbiological consequences of  
97 bleaching events can lead to total community collapse if mortality is widespread. However,  
98 some coral species, and individuals within species, are resilient to the effects of bleaching and  
99 appear to return to pre-bleaching status. Corals resilient to thermal stress can reacquire  
100 symbionts, fully recover physiological performance and yield viable gametes (e.g., 23), though  
101 the timescale for post-bleaching recovery can vary from weeks to a year (24-27). Post-bleaching  
102 recovery times may be shorter in corals that have previously been exposed to multiple annual

103 bleaching events (28), perhaps by priming the physiological responses necessary to survive  
104 bleaching.

105 There are several possible contributing factors that may provide greater coral holobiont  
106 resilience to bleaching events: host- and/or symbiont- species (29-32), host genotype (33-38),  
107 or the microbial constituents of the holobiont's microbiome (39, 40). At the center of this  
108 complex equation is the host's metabolic capacity before and after bleaching (i.e., how is the  
109 coral acquiring nutrients to sustain growth and immune function?). Without adequate carbon  
110 and nitrogen, the coral cannot maintain systems of cellular and tissue repair, retain, or reacquire  
111 symbionts, or fight off pathogens (e.g., 41, 42). This suggests that the pre-bleaching molecular  
112 physiology of the coral host may be the most important factor in determining resilience to  
113 bleaching stress and mortality.

114 The interactions between an organism and its environment are complex and depend upon  
115 ecological and evolutionary history. Corals in Hawai'i, Kāne'ohe Bay, O'ahu have endured an  
116 increased frequency of bleaching events. Results from bleaching surveys in the bay have  
117 shown a decrease in the proportion of coral colonies bleached over time (62% in 1996 to 30% in  
118 2015) but an increase in the number of colonies dying (<1% in 1996 to 22% in 2015). Kāne'ohe  
119 Bay is inhabited by the reef-building Scleractinian coral *Montipora capitata* (43). These corals  
120 are typically found in tropical waters, living within 1-2°C of their upper thermal limit (44, 45). This  
121 suggests that projected future water temperatures will specifically threaten this species (e.g.,  
122 46). *Montipora capitata* has been shown to have higher thermal tolerance than other Hawaiian  
123 coral species (47) and is thereby an ideal candidate to study the long-term effects of thermal  
124 acclimatization or adaptation to reveal the underlying molecular physiology that supports  
125 bleaching resilience.

126 In this study, we report the results of a joint coral physiology, proteomic, lipid, and microbiome  
127 analysis comparing the features of *M. capitata* coral colonies that recovered *in situ* from  
128 experimental bleaching against the features of those that died. Colonies of visually healthy *M.*  
129 *capitata* were exposed to 30°C water in experimental tanks for three weeks to simulate thermal  
130 stress and induce bleaching. Samples for proteomics, microbiome diversity, total lipids,  
131 Symbiodiniaceae density and clade diversity were collected before thermal stress (T<sub>1</sub>) and three  
132 weeks after bleaching occurred (T<sub>2</sub>) (Fig.1). A control set of the same colonies did not undergo  
133 thermal-induced bleaching. After the three weeks, corals were outplanted to the field and  
134 monitored for eight months to identify colonies that recovered from the thermal-induced  
135 bleaching event and those that died. These outcomes were then retroactively used to label the  
136 previously collected samples as deriving from *resilient* or *susceptible* colonies. The proteomic,  
137 microbial, and physiological differences uncovered in this study thus describe intraspecific  
138 differences associated with bleaching resilience in the field. Because coral colonies were  
139 collected from and outplanted to the same location at Moku O Lo'e island in Kāne'ohe Bay, they  
140 experienced the same water and thermal conditions throughout the study.

141 Comparison of resilient vs. susceptible *M. capitata* using semi-quantitative proteomics allowed  
142 the generation of metabolic maps of abundant enzymes and outlined coral's energetic priorities  
143 that may confer resilience in a changing climate. Several proteins significantly differed between  
144 resilient and susceptible colonies prior to experimental thermal stress, contributing to bleaching  
145 resilience. These resilience-associated proteins reveal dominant nutritional and metabolic  
146 strategies underpinning the ability to survive bleaching. The proteome also revealed evidence

147 for symbiont rejection, antiviral activity, enhanced immune response to pathogens, and carbon  
148 and nitrogen pathways exclusive to resilient colonies. Additional molecular-level metrics of the  
149 holobionts were monitored, including total lipids, microbiome diversity, and symbiont density and  
150 diversity, allowing us to evaluate and establish whole-organism biomarkers of resilience. These  
151 molecular-level signatures could be used to predict coral resilience or susceptibility prior to a  
152 bleaching event. Last, we report a multi-factor approach to identify the corals that will survive future  
153 bleaching events, the lynchpin to coral management, propagation efforts, and restoration success.

## 154 Results

155 In September 2017 seventy-four colonies of *Montipora capitata* were tagged (with an ID) and  
156 collected, acclimated in tanks for two weeks, sampled ( $T_1$ ), gradually exposed to increasing  
157 water temperatures to reach 30°C, and held at 30°C for three weeks to simulate a thermal  
158 bleaching event (Fig. 1). Water temperatures were returned to ambient temperatures over 4  
159 days, after 24 hrs at that temperature corals were sampled ( $T_2$ ) and then were monitored for  
160 long-term survival and recovery for eight months (Figs. 1 and S1). After three months  
161 (December), 22 colonies died; these colonies will be referred to as “susceptible”. Fifty-two  
162 colonies recovered and reacquired symbionts; these colonies will be referred to as “resilient”.  
163 After December, no coral mortality was observed. By May, all the colonies that survived reached  
164 pre-bleaching coloration (Fig. 1B). At  $T_1$  and  $T_2$ , we obtained coral samples to examine  
165 physiological performance and recovery. Six of the 52 resilient colonies and six of the 22  
166 susceptible colonies were randomly selected for the study and frozen sub-samples at both  
167 timepoints were used for mass spectrometry-based proteomics, total lipid content,  
168 Symbiodiniaceae density and diversity, and bacterial community composition.

169 At  $T_1$ , no significant difference was measured in symbiont density between the resilient and  
170 susceptible colonies (Fig. 1B, Dataset S1A). During the thermal event, the symbiont density  
171 decreased in both cohorts at the same rate; within 3 months after  $T_2$ , the resilient cohort  
172 returned to pre-bleaching Symbiodiniaceae density. Additionally, there was no significant impact  
173 of bleaching, time point, bleaching tolerance, or colony of origin on symbiont clade abundances  
174 (Fig. S1B; Dataset S1B).

175 A total of 2,193 coral proteins were identified at  $T_1$ , 2,161 coral proteins were identified at  $T_2$ ,  
176 and 1,424 coral proteins were shared between those timepoints, indicating constitutive  
177 expression (Fig. S2, Dataset S2A-G). Analysis of the resilient and susceptible colonies  
178 independent of timepoint revealed 2,276 proteins detected in the resilient cohort and 2,066  
179 proteins in susceptible colonies.

180  
181 **Biological enrichment analysis.** Enrichment analysis of Gene Ontology (GO) terms was  
182 completed using MetaGOmics (48), an unbiased method to identify significantly different  
183 metabolic processes represented in proteomes of the resilient vs. susceptible cohorts at both  
184 timepoints using log-fold change (base 2; LFC) of GO term assignments (Dataset S3A-B).  
185 Resilient colonies at  $T_1$  were characterized by multiple cellular responses to external signals,  
186 receptor activity, and monosaccharide binding. Sterol esterase activity was the most enriched  
187 term (LFC=5.0; Fig. 2A). Six GO terms were significantly enriched in susceptible colonies prior  
188 to bleaching ( $T_1S$ ) and included proteins involved in urea and amide catabolism, nickel binding,  
189 and the removal of superoxides (Fig. 2A). After thermal bleaching, 51 GO terms were enriched

190 in resilient corals, 33 of which were unique (Fig. 2B). Proteomes of resilient colonies post-  
191 bleaching (T<sub>2</sub>R) were enriched in regulation of phagocytosis and meiotic cell cycle, vesicle-  
192 mediated transport, hormone regulation, and cardiac muscle processes. Although some of the  
193 labels for these processes may not seem to apply to corals, proteins associated with the  
194 “cardiac muscle process” GO term are involved in sodium and calcium exchange while  
195 “regulation of systemic arterial blood pressure” proteins include sodium-driven chloride  
196 bicarbonate exchange proteins involved in pH regulation. Many of the identified GO terms in  
197 susceptible colonies post-bleaching involved the cellular processing of metabolites, including  
198 sterols, methionine, betaine, sarcosine, lipids, and glutamate. Additionally, several terms were  
199 related to DNA or RNA processing.

200  
201 **Immune system responses.** To elucidate complete metabolic pathways being preferentially  
202 utilized by either the resilient or susceptible colonies at the two timepoints, significant differential  
203 abundances of proteins were calculated (Fig. 2C, D; significance only reported when  $p \leq 0.05$ ;  
204 Dataset S2G-H). Comparisons of resilient and susceptible colony proteomes before the  
205 simulated thermal bleaching event (T<sub>1</sub>), revealed that resilient colonies had 39 proteins at  
206 significantly higher abundances than the susceptible cohort, whereas susceptible colonies  
207 possessed 56 proteins at significantly higher abundances (Fig. 2C). In T<sub>1</sub>R colonies, signal  
208 peptidase (LepB) yielded the highest differential abundance, followed by F-type H<sup>+</sup>-transporting  
209 ATPase subunit alpha (ATPeF1A), and a membrane attack complex component/perforin  
210 (MACPF) domain-containing protein known to lyse virus-infected and pathogenic bacterial cells.  
211 Susceptible corals before bleaching (T<sub>1</sub>) significantly increased the abundance of Fibropellin-1  
212 (EGF1), a component of the apical lamina, the surface glycoprotein melanoma-associated  
213 antigen p97 (MFI2), an enzyme involved in glycosylating proteins, alpha 1,2-  
214 mannosyltransferase (KTR1\_3), and the urea degrading enzyme urease (URE1).

215 After the colonies were bleached (T<sub>2</sub>), the resilient cohort was characterized by 108 proteins  
216 that significantly increased in abundance while the susceptible cohort significantly increased the  
217 abundance of 63 proteins (Fig. 2D). A CyanoVirin-N domain-containing protein (CVNH) was  
218 identified to have the most consistent expression across the 12 colonies tested (i.e., lowest  $p$ -  
219 value), a high LFC in the T<sub>1</sub>R proteome, and the highest LFC in T<sub>2</sub>R (Fig. 2D). Further analysis  
220 of this protein sequence against the conserved domain database revealed that it contains four  
221 CyanoVirin-N conserved domains with viricidal activity that interact with the glycoproteins on the  
222 viral envelope (49). Conversely, chitinase (CHIC), an enzyme capable of degrading chitin,  
223 exhibited the highest LFC in the susceptible corals post-bleaching (Fig. 2D), another possible  
224 indication of symbiont degradation.

225 Cluster analysis of proteins that were identified across all experiments to be significantly  
226 abundant in at least one treatment (LFC  $\geq |1|$ ,  $p$ -value  $< 0.01$ ) are represented in a heatmap that  
227 spans fifteen metabolic pathways (Fig. 3). Resilient and susceptible coral proteomes are most  
228 similar at T<sub>1</sub> (clusters 1-3, 9-12) compared to the proteomes at T<sub>2</sub> (Fig. 3). Furthermore, resilient  
229 corals prior to bleaching exhibited higher abundances of several proteins involved in anti-viral  
230 activity, immune response, and symbiosome maintenance (clusters 4-7) than susceptible corals.  
231 After thermal bleaching, the resilient coral colonies maintain a significantly higher abundance of  
232 six enzymes, including CVNH (cluster 1), compared to susceptible corals. The T<sub>2</sub>R cohort  
233 uniquely increased the abundance of 37 additional proteins (cluster 3) involved in nitrogen

234 metabolism, immune response, endosome/symbiosome activity, and DNA translation, among  
235 others. Pre-bleaching susceptible corals (T<sub>1</sub>S), despite exhibiting somewhat similar proteomic  
236 trends to T<sub>1</sub>R, revealed one unique cluster (cluster 8) of 9 proteins that were significantly  
237 increased in abundance. These proteins play a role in structures and functions such as the  
238 extracellular matrix, and immune response, or are associated with lysosome/phagosome  
239 activity. Post-bleaching susceptible corals (T<sub>2</sub>S) had the most distinct proteomic response, with  
240 depletion of nearly all proteins represented by clusters 1-8 and enrichment in a unique suite of  
241 proteins in carbon, nitrogen and lipid metabolism, the biosynthesis of secondary metabolites,  
242 the extracellular matrix, and the immune system (clusters 11-12).

243 **Resilient corals retain lipids through the thermal bleaching event.** Previous investigations  
244 on recovery from thermal bleaching events revealed that *M. capitata*, unlike other corals, has  
245 the unique ability to replenish energy reserves within 1-2 months after the bleaching event,  
246 making it one of the coral species with the fastest recovery rates (50). Pre-bleaching, resilient  
247 corals had significantly greater abundances of enzymes involved in lipid degradation compared  
248 to the susceptible cohort (e.g., PSAP and LIP, Fig. 2A). To determine if pre-bleaching lipid  
249 biomass (i.e., T<sub>1</sub>) is a significant and predictable metric to identify *M. capitata* colonies that will  
250 recover from thermal bleaching events, total lipids were measured. No significant difference in  
251 coral lipid content was found before the simulated thermal event (i.e., between T<sub>1</sub>R and T<sub>1</sub>S  
252 colonies; Dataset S1D-E). Coral lipid content varied significantly by bleaching status at T<sub>2</sub> (T<sub>2</sub>B  
253 vs. T<sub>2</sub>NB:  $p=0.00079$ ; Fig. 2F) and long-term tolerance to bleaching (T<sub>2</sub>R vs. T<sub>2</sub>S:  $p=0.00095$ ;  
254 Fig. 2E). Interaction of the two variables was also significant ( $p=0.044$ ): susceptible corals  
255 experienced a decrease in mean lipid content by 44% after exposure to thermal stress (T<sub>1</sub>S and  
256 T<sub>2</sub>S), while resilient colonies decreased by only 16% (T<sub>1</sub>R and T<sub>2</sub>R).

257 **Resilient corals have more diverse bacterial communities.** Alpha diversity of the  
258 microbiome based on the 16S rRNA V4 variable region was quantified using Faith's  
259 phylogenetic diversity (Faith's PD), a measure of microbiome richness that accounts for  
260 phylogeny. Faith's PD significantly differed among groups defined by each combination of  
261 timepoint, bleaching resilience, and bleaching status (Kruskal Wallis  $p=0.0045$ ). Prior to  
262 bleaching (T<sub>1</sub>), resilient *M. capitata* had higher alpha diversity compared to susceptible corals  
263 (Kruskal Wallis  $p=0.016$ ; Fig. 4A). However, this difference could be attributable to multiple  
264 comparisons (false discovery rate (FDR)  $q=0.061$ ). After bleaching, previously low-diversity  
265 susceptible corals exhibited significantly increased alpha diversity ( $p=0.0065$ , FDR  $q=0.048$ ),  
266 while previously high-diversity resilient corals did not ( $p=0.52$ , FDR  $q=0.6$ ). Thus, resilient corals  
267 showed smaller microbiome changes during bleaching and over time than susceptible corals,  
268 consistent with greater stability in microbiome richness.

269 Beta diversity was also quantified to determine the similarities of the bacterial communities  
270 between cohorts. Across combinations of timepoint, resilience, and bleaching status, microbial  
271 community composition differed qualitatively (Unweighted UniFrac PERMANOVA;  $p=0.002$ ) and  
272 quantitatively (Weighted UniFrac PERMANOVA;  $p=0.041$ ). These differences were not  
273 attributable to differences in microbiome dispersion (Weighted and Unweighted UniFrac  
274  $p>0.05$ ).

275 The main taxonomic drivers of community differences revealed that Gammaproteobacteria  
276 were well represented in the six resilient colonies and nearly absent in susceptible colonies (Fig.

277 4), consistent with the overall community differences detected in beta-diversity analysis. At the  
278 family level, multiple microbial families showed striking differences between the resilient and  
279 susceptible cohorts. The clearest of these differences was seen in *Moraxellaceae*, a family in  
280 class Gammaproteobacteria that was only found in resilient corals at T<sub>1</sub>. Microbiome  
281 Multivariate Association with Linear Models (51), a statistical analysis method that identifies  
282 multivariable association between microbial features and metadata (i.e., time, resilience,  
283 bleaching), confirmed that *Moraxellaceae* significantly correlated with both time and resilience  
284 (MaAsLin2<sub>TIME</sub>  $p=0.0001$ ; MaAsLin2<sub>RVS</sub>  $p=0.0007$ ; Table S1). Additionally, the *Caulobacteraceae*  
285 microbial family—in the phylum Proteobacteria—was present at elevated abundance in resilient  
286 corals, and lower abundance in susceptible ones (irrespective of timepoint or bleaching status  
287 (MaAsLin2<sub>RVS</sub>  $p=0.0006$ ).

## 288 Discussion

289 Although multiple Cnidarian species have had their proteomes analyzed (e.g., *Eunicea*  
290 *calculata* (52); *Amphistegina gibbosa* (53); *Acropora microphthalma* (54); *Acropora millepora*  
291 (55), *Montipora capitata* (56, 57)), to date, no studies have exhaustively explored pre-bleaching  
292 protein-level physiology in combination with multiple other molecular-level factors to determine if  
293 there are traits predictive of resilience to bleaching events. Despite previous research showing  
294 that symbiont clade D can lead to reduced levels of bleaching in multiple coral species or  
295 improve thermal tolerance (29, 36), these coral colonies show no significant differences in clade  
296 abundances or distributions across bleaching status, time point collected, or tolerance to  
297 bleaching (Dataset S1A, B; Fig S1B). In general, more proteins were detected in all corals at T<sub>2</sub>  
298 post-bleaching relative to T<sub>1</sub> pre-bleaching, a common response to exogenous stressors (e.g.,  
299 58-60). Simultaneous activation of multiple metabolic pathways provides bleached *M. capitata*  
300 with new carbon and nitrogen acquisition strategies as symbiont-delivered photosynthate is  
301 diminished or absent. Our primary hypothesis is that molecular phenotypic differences -  
302 resulting from genetics or epigenetics - will enhance the ability of some individual corals to  
303 mitigate the effects of bleaching. Before thermal stress occurred (T<sub>1</sub>), the only significant  
304 differences were identified in protein abundances and in the microbiome diversity between  
305 susceptible and resilient colonies. Examination of the significantly changing metabolic pathways  
306 in the resilient and susceptible cohorts reveals for the first time how nutritional strategies,  
307 antiviral mechanisms, and microbiome diversity pre-and post-bleaching dictate survival.

308 **309 Phenotypic advantages in resilient corals prior to bleaching.** Several proteins in metabolic  
310 pathways associated with maintenance of a functional symbiont- host relationship were present  
311 at increased abundance in the resilient coral proteome prior to the bleaching event. The primary  
312 active pathways that were enhanced in resilient corals pre-bleaching include sterol and lipid  
313 degradation, cellular respiration, oxidative phosphorylation, and carbon metabolism (Fig. 2A).  
314 Total lipid biomass in the resilient corals had a broader range of values and a higher average  
315 than the susceptible cohort (Fig. 2E).

316 Prior to bleaching, resilient corals utilize heterotrophic feeding and symbiont photosynthate.  
317 The GO term sterol esterase was the most significantly increased term in resilient *M. capitata*  
318 colonies. Analysis of proteins contributing to this GO term revealed the dominating contributors  
319 to the enrichment analyses included a gastric triacylglycerol lipase-like protein (LIP) (Fig. 3;

320 cluster 4) and the lipid-specific degradation enzyme saposin (PSAP; Fig. 2C). These enzymes  
321 are typically involved in digestion and likely reside in the coral gastric cavity, suggesting that at  
322 T<sub>1</sub>, pre-bleaching, the resilient corals are using a heterotrophic feeding strategy in addition to  
323 photosynthate from *Symbiodiniaceae*. This was not unexpected as *M. capitata* has been  
324 previously observed to utilize heterotrophy when not bleached (61). T<sub>1</sub> resilient corals also  
325 possessed higher abundance of early endosome antigen 1 (EEA1), an essential protein in  
326 symbiosis establishment (i.e., 62-64), providing resilient corals with an advantage for  
327 maintaining symbiont relationships compared to the susceptible corals. Utilization of diverse  
328 feeding strategies would provide a distinct advantage to the resilient corals as the excess  
329 carbon can be shuttled into lipid storage vesicles (61, 65).

330 Resilient corals present evidence of more active cellular respiration pathways at T<sub>1</sub> prior to the  
331 bleaching event. Although many enzymes in the carbon metabolism pathway are constitutively  
332 expressed in resilient and susceptible corals, the increased abundance of isocitrate lyase (ICL;  
333 Fig. 2C) provides resilient corals utilization of the glyoxylate shunt, a TCA-cycle bypass that  
334 allows cells to complete anabolic reactions with 2-carbon units without losing carbon as CO<sub>2</sub>  
335 (the opposite of what is observed in susceptible corals at T<sub>1</sub>; Fig. S3A). Further, increased  
336 abundances of glycine hydroxymethyltransferase (GLY; Fig. 2C) provides single carbon (1C)  
337 units to the cell, fueling the glyoxylate shunt for the generation of larger carbon-storage  
338 molecules (i.e., lipids) from the excess 1-2 carbon unit small molecules, again bypassing the  
339 generation/loss of CO<sub>2</sub> (66, 67). Additional evidence, such as increased abundance of pyruvate  
340 dehydrogenase (PDHa; Fig. 2C) and multiple acetyl-CoA transferases support increased  
341 cellular respiration and the potential to store excess energy in resilient corals.

342 Prior to bleaching, the resilient corals appear to prime anti-viral activity and exhibited a  
343 significantly more diverse microbiome, which likely supported their immune response. Previous  
344 demonstrations of “frontloading” immune response or pathogen-fighting enzymes have been  
345 shown to increase survival in corals (68). One of the most differentially abundant proteins that  
346 was elevated in resistant colonies at T<sub>1</sub> was a cyanovirin-like protein (CVNH; Figs. 2C), an  
347 evolutionarily conserved protein that binds to viruses and blocks entry into the cell (69). CVNH  
348 was also detected in higher abundances in the resilient cohort through T<sub>2</sub>, post-bleaching (Figs.  
349 2D and 3, cluster 1). To determine if there were identifiable viral proteins in the whole-coral  
350 protein extractions and mass spectrometry analyses conducted, the data was analyzed using a  
351 larger database that included 5 coral-associated viral proteomes (Table S2). The number of  
352 confident peptides associated with the viral proteins detected were not statistically different  
353 between resilient and susceptible colonies at T<sub>1</sub>, yet their presence in whole-holobiont protein  
354 extract does corroborate the need for corals to produce antiviral proteins. Additionally, the T<sub>1</sub>R  
355 colonies hosted a significantly more diverse microbiome (Fig. 4A), which has a positive effect on  
356 host health (70). The resilient microbiome included the *Moraxellaceae* bacterial family, which  
357 was only found in resilient coral colonies. *Moraxellaceae* are associated with local wastewater  
358 and they are known to have high numbers of antibiotic resistance genes (ARGs) (71, 72). As the  
359 coral host’s immune system is activated against pathogenic bacteria and releases antimicrobial  
360 defenses, the *Moraxellaceae* bacterial family’s high number of ARGs may provide them with an  
361 advantage for long-term residence on the host. As *Moraxellaceae* has been found to be a  
362 common component of many shallow water coral microbiomes, these bacteria may be important  
363 in shaping a healthy coral holobiont (73). The functional role of this bacterial family’s unique

364 genome in conferring resilience against bleaching to coral colonies is unknown, but the close  
365 association of *Moraxellaceae* on resilient *M. capitata* colonies merits further research.  
366

367 **Molecular signs of stress before thermal induced bleaching in susceptible corals.** A  
368 detailed proteomics analysis revealed the metabolic processes identified in susceptible corals  
369 prior to bleaching, including urea and amide catabolism, nickel binding, and urease activity (Fig.  
370 2A). Redirected nitrogen and carbon uptake pathways in susceptible corals suggest a decrease  
371 in symbiont-derived photosynthate at T<sub>1</sub>. Previous molecular-level investigations of symbiont-  
372 host relationships have demonstrated that the majority of nitrogen assimilation occurs via the  
373 symbiont-directed GS/GOGAT (glutamine synthase/glutamine oxoglutarate aminotransferase)  
374 activity or the coral host-directed glutamine synthetase or glutamate dehydrogenase activity  
375 (e.g., 74). Prior literature suggests that the majority of nitrogen uptake is from symbiont-  
376 transferred metabolites resulting from their utilization of free ammonia in the water column (e.g.,  
377 75), although it has been suggested that the assimilation of nitrogen by the host itself is  
378 underestimated (76). Here, there is evidence that the susceptible coral colonies utilized urea as  
379 their primary nitrogen source at T<sub>1</sub> (Fig. S3).

380 We propose that high levels of the urease enzyme may be a biomarker of a dysfunctional  
381 metabolic relationship between the coral host and its algal symbiont. Urea, a soluble nitrogen-  
382 rich molecule, is degraded intracellularly to yield ammonia and carbon dioxide (CO<sub>2</sub>) via urease  
383 enzyme (URE1, Fig. 2A,C and S3). At T<sub>1</sub> in susceptible corals, GO terms for nickel-binding  
384 activity and carbonic anhydrase activity are enriched (Fig. 2A). Proteins associated with these  
385 functions provide the required nickel cofactor for urease (77) and increased abundances of  
386 carbonic anhydrase enzyme (CA) rapidly converted CO<sub>2</sub>, byproducts of the reaction, into  
387 carbonic acid (or bicarbonate). It has been suggested that coral cells rely on this pathway to  
388 acquire additional nitrogen when under stress (78, 79). For example, in corals lacking  
389 Symbiodiniaceae, urease activity increased to compensate for the lack of Symbiodiniaceae-  
390 provided nitrogen (79). Previous experiments on corals revealed that urea- and nickel-  
391 enrichments increased photosynthesis and calcification rates, suggesting that these molecules  
392 support coral growth in adverse environmental conditions (77). Isocitrate dehydrogenase  
393 (ICDH1; FC: 0.57)), an enzyme that is increased under nitrogen starvation, is slightly increased  
394 in T<sub>1</sub> susceptible (compared to T<sub>1</sub>R) corals. ICDH1 links the carbon metabolism (TCA cycle) and  
395 nitrogen cycle together to generate glutamate (via GS-GOGAT; Fig. S3A). The increased  
396 presence of enzymes involved in these alternate routes of nitrogen and carbon acquisition  
397 provide molecular evidence for their use as potential biomarkers of environmental stress and/or  
398 the beginnings of dysfunctional symbiosis.

399 After thermal bleaching (T<sub>2</sub>), the abundance of urease (URE1) continues to increase and is  
400 consistently more abundant in susceptible corals at both timepoints (Fig. 3, cluster 9).  
401 Therefore, urea-dominated nitrogen acquisition strategy in the host increases as the host-  
402 symbiont relationship becomes compromised in susceptible coral colonies responding to  
403 thermal stress. Although it has been proposed that the prokaryotic host-associated microbiome  
404 could provide bioavailable nitrogen via nitrogen fixation when the host is stressed, the 16S  
405 rRNA does not provide species-level resolution that would definitively reveal if any of the noted  
406 bacterial families in T<sub>2</sub>S microbiome were nitrogen-fixers.

407 Importantly, the susceptible corals displayed early evidence for the rejection and degradation  
408 of symbiosomes in before the thermal stress starts. The coral's symbionts reside in specific  
409 phagosomes called symbiosomes; corals therefore have specific enzymatic and signaling  
410 pathways to disrupt the standard phagosome recycling mechanisms, ensuring the symbiont's  
411 residence. Typical phagosome recycling via hydrolytic enzymes is directed by Rab11  
412 expression in coral hosts (80). Established, healthy symbiotic relationships therefore inhibit the  
413 Rab11 pathway, resulting in a decrease in Rab11 abundance (e.g., 80). Susceptible corals at T<sub>1</sub>  
414 displayed significantly increased abundance of Rab11 (Fig. 2C), an early indication of a  
415 dysfunctional symbiotic relationship and potential host-directed degradation of the symbiosome,  
416 or symbiophagy (81). This host-symbiont disequilibrium hypothesis in T<sub>1S</sub> corals is further  
417 supported by increased abundance of Tubulin alpha (TUBA), a phagocytosis protein recognized  
418 to be active in symbiont degradation (82), among other functions. Three enzymes detected at  
419 significantly increased abundances were involved in glycan degradation, in particular the  
420 mechanism involved in cleaving mannose-based oligosaccharides: alpha-L-fucosidase  
421 (FUCA1), mannose-receptor (MRC1), and mannosyl-oligosaccharide alpha-1,3-glucosidase  
422 (GANAB) (Fig. 3, cluster 8). As mannose is recognized by lectin proteins in corals to identify  
423 pathogens and symbionts, the degradation of these mannose-based oligosaccharides would  
424 weaken physical associations of the host with symbionts and its microbiome (83, 84). Further,  
425 the degradation of these oligosaccharides would specifically provide easily accessed glucose  
426 monomers for supporting the energy-demands of the susceptible coral colonies at T<sub>1</sub>. Increased  
427 presence of mucin proteins (i.e., MUC4, Fig. 2C), a noted deterrent to pathogen colonization  
428 (85), and lectins, pathogen recognition proteins (e.g., TLEC2; Fig. 3, cluster 8) suggest that T<sub>1</sub>  
429 susceptible corals are being challenged by pathogens, further weakening their immune system  
430 prior to the bleaching event. The T<sub>1S</sub> microbiome was less diverse than the T<sub>1R</sub> colonies'  
431 microbiomes and more variable across the entire susceptible cohort (i.e., each T<sub>1S</sub> colony had a  
432 different taxonomic composition). Quantification of the panel of proteins listed here linked to  
433 symbiont rejection could provide coral managers with a rapid biomarker test for identifying which  
434 corals are stressed and may not be suitable for propagation, even under optimal environmental  
435 conditions.

436

#### 437 **Divergent metabolic strategies in resistant and susceptible corals post-bleaching.**

438 Constitutive post-bleaching (T<sub>2</sub>) response across all *M. capitata* included many components of  
439 the phagocytic and endocytic pathways, indicating that active symbiotic expulsion (86) during  
440 thermal stress-induced bleaching was occurring regardless of whether the corals were resilient  
441 or susceptible. In particular, Rab11, the inhibitor of symbiosome degradation observed in T<sub>1S</sub>,  
442 was detected at increased abundances in both coral groups at T<sub>2</sub> relative to the T<sub>1</sub> samples.  
443 Other constitutively expressed immune response proteins detected at higher abundances at T<sub>2</sub>  
444 included NOD, MAPK, WNT, and TOLL-like receptors. All of these signaling pathways have  
445 been previously observed in corals (87) and their detection suggests that during bleaching the  
446 innate immune system is activated. Here, we detected increased abundances of the protein  
447 responsible for the irreversible step in gluconeogenesis in susceptible corals, and increased  
448 abundances of two irreversible steps in glycolysis in the resilient corals (Fig. S3B). This  
449 proteomic evidence suggests that after bleaching, the resilient corals have a more accessible  
450 glucose source, whereas the susceptible corals are catabolizing non-carbohydrate sources,

451 such as lipids and proteins. These enzymatic pathway analyses also provide a molecular  
452 foundation for the observed 49% decrease in lipid biomass in the susceptible colonies and the  
453 insignificant change in lipids in the resilient corals between pre- and post-bleaching (Fig. 2F).  
454

455 **Resilient corals diversify metabolic pathway utilization to recover from thermal**  
456 **bleaching.** After bleaching, several GO terms were enriched in resilient *M. capitata*: amino acid  
457 synthesis (methionine, and proline), sulfur amino acid metabolic process, immune response, cell  
458 signaling/oxidoreductase, endoplasmic reticulum (ER) organization, oxoacid metabolism, and  
459 ribosome assembly (Fig. 2B). Sulfur amino acids, such as methionine, are antioxidants and  
460 therefore capable of providing oxidative protection to cells (88). Increased levels of these amino  
461 acids in resilient corals could be indicative of increased need for protection against oxidative  
462 stress resulting from the heat. Sulfurtransferase enzymes are present in both susceptible and  
463 resilient corals, however they are significantly increased in resilient corals (Fig. 3, clusters 1 and  
464 2). Heat stress has been found to also induce an increase in endoplasmic reticulum transcripts  
465 in *Acropora hyacinthus* (89), mirroring our findings of increased abundance of ER proteins.  
466 Increases in cell signaling and ribosome assembly proteins are likely indicative of more normal  
467 cellular trafficking in healthy host tissue, enabling recovery from thermal bleaching. Several  
468 metabolic pathways are discussed below that support the resilient metabolism through thermal  
469 stress compared to the susceptible coral cohort.

470 Resilient corals activate endocytic uptake pathways and heterotrophic feeding after bleaching  
471 event to aid in nutritional recovery. Multiple enzymes involved in endocytosis are increased in  
472 the T<sub>2</sub>R cohort providing a heterotrophic avenue for carbon and nitrogen acquisition (Fig. 3,  
473 cluster 3). Increased abundance of 2 tubulin alpha proteins (TUBA), vacuolar sorting endocytic  
474 protein (VPS4), dynamin and coatamers (COPG, COPB2) imply increased endocytic activity  
475 of particles, such as pathogens or food (82, 90). Significantly increased abundance of lysosome  
476 associated membrane protein (LAMP) may indicate that symbiont engulfment and degradation  
477 is an additional potential source of nutrition for resilient corals post bleaching (81). Significantly  
478 increased peptide degradation enzymes in the T<sub>2</sub>R cohort included glutamyl amino peptidase  
479 (ENPEP, (Fig. 3, cluster 3), which cleaves acidic amino acids from the N-terminus of peptides  
480 for subsequent degradation to enhance cellular growth. T<sub>2</sub>R also significantly increased a  
481 vitellogenic carboxypeptidase (CPVL), a protein involved in the degradation of yolk proteins.  
482 This may be a sign of a physiological switch to sacrifice reproductive potential to increase the  
483 chances of bleaching recovery and short-term survival. Abundant protease/peptidases (Fig. 3,  
484 cluster 3) and lipases (e.g., triacylglycerol lipase PNLLIP; Fig. 2D) in resilient colonies can break  
485 the bonds of macromolecular complexes to generate mobile small molecules that can be  
486 recycled or further degraded for energy. In support of these findings suggesting adequate  
487 nutritional resources were available in the resilient cohort post-bleaching, the increased  
488 abundance of transketolase (TKT) in T<sub>2</sub>R may indicate a higher abundance of thiamine (vitamin  
489 B1) compared to T<sub>2</sub>S (91, 92).

490 To further aid in recovery, resistant corals post bleaching appear to utilize several new  
491 pathways to aid in cellular nitrogen and carbon demands. Although the urea degrading enzyme  
492 URE1 is detected in both T<sub>2</sub>S and T<sub>2</sub>R corals, T<sub>2</sub>R displayed increased abundance of polyamine  
493 oxidase (MPAO; Fig. 3 cluster 3) which may allow resilient colonies to access polyamine-  
494 nitrogen as needed and produce beta-alanine. Beta-alanine (aminopropanoic acid) is a  
495 degradation product of the nucleotide uracil and is a precursor to acetyl-CoA. Notably, it has

496 been found to increase cellular oxygen consumption and respiration rates (93). Detecting  
497 multiple enzymes involved in these pathways to be at significantly higher abundance in the T<sub>2</sub>R  
498 colonies provides a molecular explanation for hypothesized improved energy production  
499 compared to the T<sub>2</sub>S colonies when symbiont derived photosynthate is diminished. Further, this  
500 energy may have provided resilient colonies the ability to significantly increase multiple  
501 enzymes responsible for DNA transcription and translational processes (Fig. 3, cluster 3).

502 T<sub>2</sub>R also launched an antiviral campaign during thermal stress to assist the immune system.  
503 Cyanovirin protein (CVNH) was detected in resilient corals at T<sub>1</sub> and T<sub>2</sub> at three-fold higher  
504 abundance, compared to susceptible colonies (Fig. 3, cluster 1). Although we do not believe this  
505 to be the only mode of protection for the resilient cohort, high production of this protein could  
506 increase the resilience of these corals after bleaching events when they are simultaneously  
507 coping with multiple stresses.

508 **Catastrophic metabolic choices in T<sub>2</sub>S corals.** GO term enrichment analysis revealed a  
509 greater abundance of proteins participating in peptide degradation and protein transport in  
510 susceptible *M. capitata* post-bleaching (Fig. 2B,D; Fig. 3 cluster 12). Since Symbiont-derived  
511 photosynthate nutrition is absent in the bleached corals, susceptible colonies may have  
512 increased mobilization and degradation of proteins and peptides to provide the needed energy  
513 for cellular maintenance. Decreases in the free amino acids pool resulting from protein  
514 degradation in thermally bleached *Acropora aspera* suggests that these amino acids are being  
515 metabolically leveraged to provide energy during low photosynthate yield (94).

516 Specifically, susceptible hosts post-bleaching express an abundance of enzymes that suggest  
517 host-directed catabolism of remaining symbionts. Several lysosomal-targeted  
518 peptidases/degradation enzymes were significantly increased in the susceptible corals in  
519 response to bleaching (e.g., cathepsin CATL, galactosidase GLB, and Niemann Pick C2 protein  
520 NPC2, Fig. 3, clusters 7, 12). The early signs of a weakened host-symbiont relationship for T<sub>1</sub>S  
521 corals (discussed earlier) appears to have progressed further in the susceptible cohort by T<sub>2</sub>. At  
522 T<sub>2</sub>, health-compromised/dead symbionts may be leaking organic substrates that are degraded  
523 by lysosomal and intracellular peptidases and hydrolase enzymes (Fig. 3, cluster 12). NPC2  
524 enzymes are concentrated in the symbiosome and participate in the direct sterol transfer from  
525 symbionts (95). Evidence of increased host-directed transfer of sterols from the symbiont  
526 combined with increased lysosomal-catabolic processes indicate that after bleaching, the  
527 symbiosome and its contents are targeted for rapid degradation in susceptible colonies (81).

528 Further, the decrease in symbiont-derived photosynthate in susceptible corals leads to  
529 activated gluconeogenesis and the degradation of glycine betaine. Glucose is one of the  
530 primary carbon molecules transferred to holobionts in cnidarian dinoflagellate symbiosis (96,  
531 97). The increased abundance of the irreversible enzymes pyruvate carboxylase (PC) and  
532 phosphoenolpyruvate carboxykinase (PCK1) in susceptible corals reveals that gluconeogenesis  
533 (i.e., the generation of glucose from pyruvate) is more active than glycolysis (i.e., the  
534 degradation of glucose; Fig. S3B). Increased abundance of these enzymes suggests that  
535 susceptible corals are more glucose-limited compared to the resilient corals after bleaching  
536 events. Gluconeogenesis depends on the catabolism of amino acids, glycine betaine, and lipids  
537 (Fig. 3, cluster 12). Lipid degradation is evidenced by the significant decrease in total lipid  
538 biomass between T<sub>1</sub>S and T<sub>2</sub>S colonies (Fig. 2E-F). Only recently were glycine betaines  
539 recognized to be a major reservoir of nitrogen for corals and the near-complete glycine betaine

540 catabolic and biosynthesis pathways have been uncovered in several genomes of cnidarians  
541 (refs within:, 98). T<sub>2</sub>S corals increased abundance of the betaine-degrading enzymes betaine-  
542 homocysteine S-methyltransferase (BHMT), glycine N-methyltransferase (GNMT), and  
543 sarcosine dehydrogenase (SARDH). Ngugi et al., (98) suggest that glycine betaines are  
544 abundant nitrogen reservoirs that are easily degraded into other nitrogen compounds such as  
545 amino acids.

546 Susceptible coral proteomes post bleaching also revealed a trend of potential decreased  
547 immune function at T<sub>2</sub>. Immune pathways results indicate that the NOD, MAPK, and TOLL-like  
548 signaling pathways are suppressed in T<sub>2</sub>S corals ( $p<0.10$ ; Dataset S2H). The suppression or  
549 inactivation of these important immune pathways may make the corals vulnerable to disease  
550 and colony mortality. The suppressed beta diversity in T<sub>2</sub>S corals reveals a shift to a less  
551 diverse symbiotic bacterial community, which may be an indicator of the onset of infection (refs  
552 within:, 99). Susceptible *M. capitata* colonies also increased tyrosinase (TYR), an indicator of  
553 immune response to an infection (100) or neutralization of reactive oxygen species (101)  
554 demonstrating that T<sub>2</sub>S corals are being challenged.

## 555 Coral management and restoration applications

556 As the ultimate goal for coral management is to be able to predict resilient coral phenotypes  
557 before investing time and money in restoration, a rapid assay to determine health status is  
558 needed. Here we presented three significant differences in the resilient and susceptible coral  
559 colonies before the thermal bleaching to forecast long-term health through thermal events:  
560 proteins (Fig 2A,C), lipids (Fig. 2E), and microbiome diversity (Fig. 4A). Previous work on corals  
561 has revealed that decreases in lipid content and in microbiome diversity can be associated with  
562 a range of environmental responses and are not exclusively associated with susceptibility to  
563 bleaching stress. Here we propose a protein-based assay to predict resilience and capture more  
564 informative results on the molecular-level health of *M. capitata*. We have identified seven  
565 proteins that could be quantified in corals before bleaching events as a resilience-based assay  
566 to select colonies for propagation or other management strategies (Fig. 5). If using mass  
567 spectrometry, quantifying five peptides through the detection of  $\geq 5$  diagnostic fragment ions  
568 from each of these proteins would provide the user with high confidence on both positive and  
569 negative signals of pre-bleaching resilience. This short list could also be expanded to generate  
570 a 60 minute assay with up to 250 peptides that are simultaneously monitored, providing further  
571 information on heterotrophic feeding/lipid degradation (i.e., LIP, PSAP), antiviral activity (i.e.,  
572 CNVH), symbiophagy (i.e., RAB11, TUBA), pathogen recognition (i.e., TLEC), mucin proteins  
573 (i.e., MUC4), urea degradation (i.e., URE1), and mannose degradation (i.e., FUCA1, MRC1,  
574 GANAB). Alternatively, selected proteins identified here as resilience biomarkers could be  
575 developed into a hand-held rapid antigen test with multiple test and control lines that could be  
576 assessed in the field on rice-grained size coral tissue samples.

## 577 Concluding Remarks

578 This is the first study to use an analytical toolbox that included mass spectrometry-based  
579 proteomics, 16S rRNA analyses of the microbiome, total lipids, and symbiont density and  
580 diversity to identify intrinsic differences that confer recovery and survival in corals before thermal

581 bleaching events. This study is also unique in that the *Montipora capitata* coral colonies had  
582 unexpected, yet vastly different, outcomes from the thermal bleaching event despite identical  
583 environmental histories and, to the best of our knowledge, coral genotypes. Our intent was to  
584 reveal a multi-factor molecular-level approach for confidently identifying resilient and susceptible  
585 coral colonies so that environmental managers could rapidly select quality candidates for  
586 propagation while in the field. Despite monitoring a range of physiological and molecular  
587 metrics, very few significant differences were discovered in the study that could positively  
588 identify resilient colonies before a thermal bleaching event. Despite lipids being a tractable  
589 metric in the field, the differences in the resilient vs. susceptible coral lipids were only present  
590 after the thermal bleaching event, making lipids ineligible as a biomarker for long term survival  
591 *prior* to thermal stress. Additionally, lipids are non-specific biomarkers since their levels are  
592 often influenced by a variety of physiological factors (*i.e.*, infection, reproduction, tissue  
593 thickness, etc.). Promising and distinct differences observed in the 16S rRNA analysis of  
594 bacterial diversity revealed that the resilient cohort hosted a significantly more diverse  
595 microbiome before the thermal event. Although microbiome diversity could aid as a metric for  
596 selecting healthy, robust coral colonies, microbiome stability and diversity can be linked to water  
597 chemistry (102), temperature (14), and short or long term diseases (103, 104). Additional  
598 research needs to be conducted to determine if specific microbial clades are significantly  
599 correlated to coral recovery and resilience through thermal induced bleaching and what  
600 functional roles they play. Quantitative proteomics analyses identified proteins that were  
601 significantly different in the two cohorts before the bleaching event, that could 1) allow confident  
602 predictions in selection of resilient over susceptible colonies and 2) reveal specific molecular  
603 advantages in the form of active pathways and primed immune responses that allow resilient *M.*  
604 *capitata* corals to survive the thermal stress despite the expulsion of *Symbiodiniaceae*. Resilient  
605 corals have a significantly higher abundance of antiviral proteins and express multiple enzymes  
606 involved in a diverse range of carbon and nitrogen acquisition such as lipid degradation,  
607 heterotrophic feeding, and respiration. Conversely, colonies that did not survive thermal  
608 bleaching had pre-bleaching molecular markers at elevated abundances that play an active role  
609 in symbiont rejection, pathogen recognition, and mannose and urea degradation. The proteins  
610 represented in each of these pathways and cellular mechanisms can be fully developed into  
611 rapid molecular assays to help assess corals and guide mitigation strategies deployed by reef  
612 management.

## 613 METHODS

614 **Coral Colony Collection and Experiment.** Seventy-four coral colonies of *Montipora capitata*  
615 (approximately 30 cm in diameter) were collected from Moku O Lo'e island (patch reef) located  
616 in Kāne'ohe Bay, O'ahu, Hawai'i (21.428°N, 157.792°W) in August 2017. Colonies were brought  
617 to shore and acclimated in flow-through outdoor tanks at the Hawaii Institute of Marine Biology  
618 (HIMB) for two weeks. At the time of collection, colonies were divided in two pieces to compare  
619 physiological performance for the same genotypes with/without exposure to thermal stress (Fig.  
620 1). In September, one half of each coral colony was exposed to warmer water temperatures to  
621 simulate a natural thermal bleaching event (56). To reach the 30°C temperature goal for the  
622 bleaching treatment, experimental tank temperatures were increased 2°C per day (1°C every 12  
623 hours) for four days. The colonies were rotated once a week between tanks to minimize tank

624 effects. For the bleaching experiment, *M. capitata* colonies were kept at this elevated  
625 temperature for three weeks to induce complete coral bleaching in all the colonies. After  
626 bleaching occurred, the tank temperature was lowered, following the previously described rate,  
627 back to ambient temperature (22°C) and subsamples of coral were taken. The coral halves that  
628 were not exposed to thermal stress remained at 25°C and were also rotated within the tank to  
629 minimize tank effects. Then, all corals (bleached and not bleached) were placed on racks off  
630 HIMB to monitor survival and physiological recovery *in situ* for eight months. Bleaching  
631 assessments were conducted on all colonies every week using the Coral Watch Card (The  
632 University of Queensland, Australia), along with assessments of mortality (Fig. S1A). Colonies  
633 that bleached and recovered were deemed to be part of the resilient cohort while colonies that  
634 bleached and died were deemed susceptible to bleaching. All resulting proteomic search  
635 results, protein accession numbers and annotation files, lipid data, symbiont density and clade  
636 data, chlorophyll data and R code for plot generation and data analysis have been deposited in  
637 GitHub (<https://github.com/Nunn-Lab/Publication-coral-resilience>).

638 Branches from twelve *M. capitata* colonies were collected at two time points: 1) in September  
639 after temperature acclimation in the tanks but before colonies were bleached ( $T_1$ ) and 2) in late  
640 September, 24 hours after bleached colonies were gradually returned to ambient temperature  
641 ( $T_2$ ). All coral samples were collected 1 cm from the tip of a branch and snap frozen immediately  
642 in liquid nitrogen. Frozen samples were shipped to the University of Washington on dry ice and  
643 stored at -80°C. Samples for protein extraction consisted of 2 mm thin cross-sections of the  
644 branches, encompassing both tissue and skeletal matrix.

645  
646 **Symbiont and Chlorophyll analyses.** Chlorophyll a concentrations and dinoflagellate symbiont  
647 (Symbiodiniaceae) densities from each of the colonies were investigated (Dataset S1A). Briefly,  
648 chlorophyll a was extracted with 100% acetone and absorbance was measured with a light  
649 spectrophotometer (Dataset S1B). Symbionts were separated from triplicate ground coral tissue  
650 by centrifugation and symbiont pellets were homogenized prior to being counted using a  
651 hemocytometer. Chlorophyll a and symbiont densities were standardized to grams of ash-free  
652 dry weight (gdw) of coral tissue (Dataset S1A,C). In order to assess the ratio of  
653 Symbiodiniaceae C and D clades a 4mm piece of frozen *Montipora capitata* was crushed using  
654 a frozen mortar and pestle and total DNA was extracted and Quantitative Real Time PCR  
655 (qPCR) assay of the symbionts' actin genes was used to determine the ratio of  
656 Symbiodiniaceae C and D clades (Dataset S1B, Fig. S1B). Further details found in SI Methods.

657  
658 **Lipid Analyses.** Total lipids were analyzed on each sample following the methods of Rodrigues  
659 and Grottoli (50). Briefly, whole fragments (tissue plus skeleton) were crushed and digested in a  
660 2:1 chloroform:methanol solution, sequentially washed in a 0.88% KCl solution, dried under  
661 grade 5.0 N<sub>2</sub> gas to a constant weight (Dataset S1D-E)

662  
663 **Proteomics.** Six colonies from the resilient cohort and six colonies from the susceptible cohort  
664 were randomly selected as bioreplicates to track phenotypic differences in protein abundance  
665 through time (*i.e.*,  $T_1$  and  $T_2$ ). Details can be found in SI Methods. Briefly, proteins were  
666 extracted from whole coral fragments (4 mm diameter x 1 mm thick, tissue plus skeletal matrix)  
667 and resulting protein concentrations were determined with bicinchoninic acid (BCA) Protein

668 microplate assay. Protein lysates (50 $\mu$ g per coral sample) were reduced, alkylated, and  
669 digested Trypsin (modified porcine sequencing grade trypsin; Promega; 1:20 enzyme:coral  
670 protein). Each digested peptide sample was amended with Peptide Retention Time Calibration  
671 Mixture (PRTC; Pierce) such that 50 fmol of PRTC was analyzed with 1  $\mu$ g of coral peptides for  
672 each mass spectrometry experiment.

673 *M. capitata* samples were analyzed using liquid chromatography coupled to tandem mass  
674 spectrometry (LC–MS/MS) on a Q–Exactive–HF (Thermo Scientific) in Data Dependent  
675 Acquisition (DDA) Top 20 mode. Samples were separated using a heated (50°C) 40 cm long  
676 analytical column packed with C18 beads (Dr. Maisch HPLC, Germany, 0.3  $\mu$ m, 120 $\text{\AA}$ ).  
677 Peptides were chromatographically separated on a Waters nanoAcuity UPLC using an  
678 acidified (0.01% formic acid) acetonitrile:water gradient of 2–45% over 120 minutes. Internal  
679 and external standards were monitored to ensure peptide peak area correlation variances were  
680 <10% through the duration of the analyses. Data was searched against a translated *M. capitata*  
681 transcriptome (105) GSE97888\_Montiporacapitata\_transcriptome.fasta). Protein identifications  
682 from the whole-cell lysates are reported if two or more peptides were identified, at least one  
683 terminus was tryptic, and the false discovery rate <0.01 (Dataset S2A-E). Differential relative  
684 protein abundances for resilient vs. susceptible corals were determined for each timepoint (T<sub>1</sub>  
685 and T<sub>2</sub>) using the QPROT-QSPEC package (106)(Dataset S2G-H). Differential abundances of  
686 proteins are reported with the following *p*-value cutoff rules: 1) *p*<0.10 if several proteins within a  
687 pathway, 2) *p*<0.05 if significance of an individual protein, or 3) *p*<0.01 if identifying a potential  
688 biomarker.

689  
690 **MetaGOMics Biological Enrichment Analysis.** To determine if categories of proteins were  
691 enriched in the resilient vs. susceptible coral cohorts at the two timepoints, a biological  
692 enrichment strategy that analyzes Gene Ontology (GO) categorical terms was used to compare  
693 sets of detected proteins (48). Top results are reported with a cutoff E-value <1E-10. A fasta file  
694 of all *M. capitata* protein sequences confidently identified in these experiments (File S3) was  
695 analyzed with MetaGOMics v.0.1.1. Although MetaGOMics was designed to analyze  
696 microbiomes, the use of the software was modified to work with a single organism by ignoring  
697 the taxonomic enrichment analysis to instead examine functions that are significantly enriched  
698 or depleted in pairwise comparisons of coral cohorts. Additional details found in SI Methods.  
699

700 **Microbiome 16S rRNA Analyses.** Total DNA was extracted from the corals selected for this  
701 study (n=12) using the Qiagen DNA extraction kit. All 16S rRNA gene amplicon sequence data,  
702 processing steps and code for quality control on the microbiome data and analysis are available  
703 on GitHub ([https://github.com/tanyabrown9/Resilient\\_vs\\_Susceptible\\_Mcapitata](https://github.com/tanyabrown9/Resilient_vs_Susceptible_Mcapitata)). Sequences  
704 are deposited in NCBI as bioproject PRJNA933787. Initial sequencing resulted in a collection of  
705 2,472,819 total reads, with an average read depth of 68,689 ( $\pm$  28,107 SD) sequences per  
706 sample (Dataset S4A-B). Amplicon sequence data were processed using the QIIME2 software  
707 package (107). Alpha diversity was assessed using the number of unique observed ASVs in  
708 rarefied samples by the Simpson's Evenness and Shannon's Diversity Indexes. Overall  
709 differences in alpha diversity across susceptibility and time points were tested using Kruskal-  
710 Wallis tests. Post-hoc comparisons were performed within each group as well as combined  
711 comparisons with *p*-values for pairwise tests between treatments adjusted for multiple

712 comparisons using Bonferroni correction. Beta diversity was assessed between samples using  
713 Weighted UniFrac distances and Bray-Curtis dissimilarities. The significance of differences in  
714 beta-diversity between susceptibility and time was tested using PERMANOVA (108). The top 10  
715 bacterial families in each sample type were selected for taxonomic analysis. Significant  
716 differences between bacterial families, susceptibility, and timepoint were carried out using a  
717 nested ANOVA. Multivariate Association with Linear Models was performed on the 16S data  
718 using the R package MaAsLin2 (51). Additional details can be found in SI Methods.

## 719 Data, Materials, and Software Availability

720 All raw MS proteomic data and protein FASTA files used for searching can be accessed at  
721 PRIDE accession PXD021262 (UsernameXXXX). All resulting proteomic search results,  
722 protein accession numbers and annotation files, lipid data, symbiont density and clade data,  
723 chlorophyll data, and R code for plot generation and data analysis have been deposited in  
724 GitHub (<https://github.com/Nunn-Lab/Publication-coral-resilience>). All 16S rRNA gene amplicon  
725 sequence data, processing steps, and code for quality control on the microbiome data and  
726 analysis are available on GitHub as well  
727 ([https://github.com/tanyabrown9/Resilient\\_vs\\_Susceptible\\_Mcapitata](https://github.com/tanyabrown9/Resilient_vs_Susceptible_Mcapitata)). All study data are  
728 included in the article and/or as SI Datasets. All sequences used in this study are publicly  
729 available through NCBI GenBank and ProteomeXchange PRIDE. Accession numbers and  
730 annotations are provided as supplementary files (Datasets S1-3).

731

## 732 Figures

733 **Fig. 1A:** Total cell counts ( $\times 10^9$ ) for Symbiodiniaceae per  $\text{gdw}^{-1}$  ( $n=6$  for each point) illustrating the  
734 experimental design to track effects of thermally induced bleaching on 12 *Montipora capitata* colonies that  
735 were monitored for 8 months. After 8 months, each colony was retroactively labeled and 6 colonies that  
736 reacquired symbionts and recovered (green) and 6 colonies that were susceptible to thermal stress  
737 (purple) were characterized. Symbiodiniaceae density for the (A) control cohort maintained at ambient  
738 (25°C) temperature and (B) experimental cohort that underwent thermally induced bleaching (30°C) for 4  
739 weeks; light green: ( $n=6$ ) resilient colonies reacquired symbionts and recovered post-bleaching; light  
740 purple: ( $n=6$ ) colonies susceptible to thermally induced bleaching that did not recover. Coral sub-samples  
741 were collected before ( $T_1$ ) and after exposure to thermal stress ( $T_2$ ) to assess host performance and  
742 symbiont and microbial composition in corals. Note that resilient and susceptible colonies were identified  
743 three months later (December); after this period no additional mortality was observed.

744 **Fig. 2.** Quantitative molecular data on proteins A-D and lipids E-F, completed on the same 12 colonies  
745 used throughout the study ( $n=6$  susceptible,  $n=6$  resilient). A and B) Volcano plots depicting -Log (p-  
746 value) vs the Laplace corrected Log Fold Change (LFC) for protein-associated Gene Ontology terms.  
747 Colored dots signify GO terms that were statistically significantly different between resilient and  
748 susceptible corals (Laplace corrected Log fold  $\leq -0.5$  or  $\geq 0.5$  and  $p$ -value  $\leq 0.01$ ). A) T<sub>1</sub> with negative LFC  
749 indicating proteins more abundant in resilient corals (T<sub>1</sub>R) while positive values correspond to proteins  
750 that were at higher abundance in susceptible corals (T<sub>1</sub>S). B) T<sub>2</sub> where negative LFC indicates greater  
751 abundance in resilient (T<sub>2</sub>R) *M. capitata* while GO terms with positive values are higher in susceptible  
752 corals (T<sub>2</sub>S). C and D) Volcano Plots of individual protein abundances. LFC  $\leq -0.5$  are proteins that were  
753 detected in significantly higher abundance in the resilient coral cohorts (green) at C) T<sub>1</sub> and D) T<sub>2</sub>. LFC  $\geq$   
754 0.5 are proteins that were detected in higher abundance in the susceptible coral cohorts (purple) before  
755 thermal-stress-induced bleaching (C: T<sub>1</sub>) and after (D: T<sub>2</sub>). E and F) Average lipid biomass (g/g dry  
756 weight) measurements on all resistant (green) and susceptible (purple) samples from the different cohorts  
757 at E) T<sub>1</sub> before bleaching and F) T<sub>2</sub> after bleaching (grey boxes) and non-bleached controls maintained at  
758 25°C (light green and purple “NB” boxes).

759 **Fig. 3.** Clustered heatmap of the subset of proteins identified to have a log fold change  $\geq 1$  or  $\leq -1.0$  ( $p$   
760  $<0.05$ ) in time point comparisons: T<sub>1</sub>R vs. T<sub>1</sub>S or T<sub>2</sub>R vs. T<sub>2</sub>S. Heatmap shades of blue indicate averaged  
761 NSAF values for bioreplicates per condition, normalized by the row mean. Rows are clustered using a  
762 correlation algorithm and a dendrogram was set to cut 12 distinct clusters (indicated by #s 1-12 black).  
763 Right panel dot-matrix indicates metabolic categories identified through KEGG, UniProt and GO (D) viral  
764 defense or (R) reproduction, CO<sub>2</sub> or as a substrate (CO<sub>2</sub><sup>-</sup>) or product (CO<sub>2</sub><sup>+</sup>), or Ca- binding domain (i.e.,  
765 Ca-binding).

766 **Fig. 4.** Phylum-level distribution of bacteria identified in resilient and susceptible colonies based on 16S  
767 rRNA sequencing data for A) T<sub>1</sub> (T<sub>1</sub>R: dk green, T<sub>1</sub>S: dk purple), B) T<sub>2</sub> after thermal stress (T<sub>2</sub>R: grey with  
768 green outline, T<sub>1</sub>S: white with dk purple outline), and C) T<sub>2</sub> control (NB) samples not exposed to thermal  
769 stress (NBT<sub>2</sub>R: It green, NBT<sub>2</sub>S: It purple). Colony ID numbers are listed on the x-axis. These same 12  
770 colony IDs were used for all analyses presented. Size of the dot represents the log transformation of the  
771 phylum-level counts.

772 **Fig. 5.** Heatmap of significantly different proteins ( $p < .01$ ) identified between resilient and susceptible  
773 corals at T<sub>1</sub>, pre-bleaching event. Colors depict NSAF values for each of the twelve coral bioreplicates,  
774 normalized by row mean. Clustered dendograms were completed with the correlation algorithm on the x  
775 and y axis to generate groups for significantly increased or decreased abundances in the resilient vs.  
776 susceptible cohorts.

777

## 780 Supplemental Information

781 **Fig. S1.** A. Bleaching assessments were completed on all colonies every week using the Coral  
782 Watch Card where 1 indicates bleached, but not dead and 6 indicates the highest symbiont  
783 density. Noted times of T1 and T2 indicate when samples were collected for this study. B.  
784 Proportion of clade C (blue) and D (yellow) identified from Resilient (greens;  $n=6$ ) and  
785 Susceptible (Purple;  $n=6$ ) coral colonies at timepoint 1 (pre-bleaching) and timepoint 2 (NB-  
786 nonbleached cohort, B- thermally bleached cohort). No statistical differences were identified  
787 using ANOVA related to bleaching status, bleaching tolerance, or timepoint.

788

789 **Fig. S2.** Venn Diagram of proteins confidently Identified in resilient ( $n=6$ ) and susceptible coral  
790 colonies ( $n=6$ ) investigated at A. timepoint 1 before thermally bleached, B. timepoint 2 after  
791 thermal bleaching, and C. the overlap of all 4 treatments and timepoints.  
792

793 **Fig. S3.** Illustration of the proteins identified to be significantly increased in abundance in  
794 resilient (greens) or susceptible (reds) coral cohorts involved in the interconnected biochemical  
795 pathways of glycolysis/gluconeogenesis, the TCA cycle, urea degradation, and the glutamine  
796 synthase/glutamine oxoglutarate aminotransferase (GS/GOGAT) pathway at A. timepoint 1  
797 before thermally bleached and B. timepoint 2 after thermal bleaching. Image was made using  
798 BioRender.  
799

800 **Fig. S4.** Graphical illustration of a multiple sequence alignments of protein  
801 Icllc238733\_g2\_i2|m.24867, noted to be significantly more abundant in the resilient colonies.  
802 The top query sequence in red (Query\_59870) represents the input sequence mentioned. The  
803 next two sequences are from *Acropora millepora* and *Mucilaginibacter sp.* MYSH2 (both in red).  
804 Multiple alignment results revealed four highly conserved CyanoVirin-N domains (CVNH: 95%  
805 Query coverage; e-value 2e-30) depicted in grey.  
806

807 **Dataset 1.** Physiological metrics on coral colonies from the study including: a readme file,  
808 symbiont density, symbiont clade distributions, chlorophyll a concentrations, lipid raw data, and  
809 lipid biomass data.

810 **Dataset 2.** Processed proteomic data on each experiment in a range of formats: a readme file,  
811 proteins identified per experiment, Normalized Spectral Abundance Factors (NSAF) on all valid  
812 proteins identified, an accession number-based annotation file, QSPEC results for timepoints 1  
813 and 2, ABACUS output file before processing.

814 **Dataset 3.** MetaGOMics output files including: a readme file, MetaGOMics results from analysis of  
815 resistant vs. susceptible coral proteins identified at timepoint 1, MetaGOMics results from analysis of  
816 resistant vs. susceptible coral proteins identified at timepoint 2.

817 **Dataset 4.** Microbiome sequence counts, metadata, and mapping information.  
818

819 **File S1.** Fasta files of protein sequences predicted from transcriptome for *Montipora capitata* plus  
820 contaminant protein database.

821 **File S2.** Fasta files of protein sequences predicted from transcriptome for *Montipora capitata* plus  
822 contaminant protein database and 5 viral proteomes (see Table S1).

823 **File S3.** Fasta file of all identified protein sequences from these experiments that were used as input for  
824 MetaGOMics analysis.  
825

826 **Table S1.** Resulting table from MaAsLin2 analysis.

827 **Table S2.** Table of coral viral proteomes selected, location the database was found, and the number of  
828 proteins downloaded.  
829

830 **Acknowledgments**

831 We would like to thank the Gates Coral Lab for hosting and supporting us during this experiment  
832 at the Hawai'i Institute of Marine Biology. We thank Brenner Wakayama, Gavin Kreitman,

833 Melissa Jaffe, and Sean Frangos for their help with collecting and culturing the experimental  
834 corals. Work was supported in part by the University of Washington's Proteomics Resource  
835 (UWPR95794), by NSF IOS-IEP 1655682 awarded to B.L.N. and J.L.P.G., NSF IOS-IEP  
836 1655888 to L.J.R., NSF GFRP awarded to J.B.A., NIH-F31 awarded to M.M and Alfred P. Sloan  
837 Research Fellowship to J.L.P.G. and by C.C.N (private funds to support environmentally  
838 relevant research aimed at making a difference) to B.L.N.  
839  
840

## 841 References

- 842 1. Mumby PJ, *et al.* (2008) Coral reef habitats as surrogates of species, ecological  
843 functions, and ecosystem services. *Conservation Biology* 22(4):941-951.
- 844 2. Salvat B (1992) Coral reefs—a challenging ecosystem for human societies. *Global  
845 environmental change* 2(1):12-18.
- 846 3. Hughes TP, *et al.* (2003) Climate change, human impacts, and the resilience of coral  
847 reefs. *science* 301(5635):929-933.
- 848 4. Pandolfi JM, *et al.* (2003) Global trajectories of the long-term decline of coral reef  
849 ecosystems. *Science* 301(5635):955-958.
- 850 5. Hoegh-Guldberg O, *et al.* (2007) Coral reefs under rapid climate change and ocean  
851 acidification. *science* 318(5857):1737-1742.
- 852 6. De'ath G, Lough JM, & Fabricius KE (2009) Declining coral calcification on the Great  
853 Barrier Reef. *Science* 323(5910):116-119.
- 854 7. Hughes TP, *et al.* (2017) Global warming and recurrent mass bleaching of corals. *Nature*  
855 543(7645):373-377.
- 856 8. Reaser JK, Pomerance R, & Thomas PO (2000) Coral bleaching and global climate  
857 change: scientific findings and policy recommendations. *Conservation biology*  
858 14(5):1500-1511.
- 859 9. Wellington GM, *et al.* (2001) Crisis on coral reefs linked to climate change. *Eos,  
860 Transactions American Geophysical Union* 82(1):1-5.
- 861 10. Muscatine L, Falkowski P, Porter J, & Dubinsky Z (1984) Fate of photosynthetic fixed  
862 carbon in light-and shade-adapted colonies of the symbiotic coral *Stylophora pistillata*.  
863 *Proceedings of the Royal Society of London. Series B. Biological Sciences*  
864 222(1227):181-202.
- 865 11. Perez SF, Cook CB, & Brooks WR (2001) The role of symbiotic dinoflagellates in the  
866 temperature-induced bleaching response of the subtropical sea anemone *Aiptasia  
867 pallida*. *Journal of Experimental Marine Biology and Ecology* 256(1):1-14.
- 868 12. Grottoli AG, *et al.* (2018) Coral physiology and microbiome dynamics under combined  
869 warming and ocean acidification. *PLoS one* 13(1):e0191156.
- 870 13. Bourne D, Iida Y, Uthicke S, & Smith-Keune C (2008) Changes in coral-associated  
871 microbial communities during a bleaching event. *The ISME journal* 2(4):350-363.
- 872 14. Lima LF, *et al.* (2020) Modeling of the coral microbiome: the influence of temperature  
873 and microbial network. *Mbio* 11(2):e02691-02619.
- 874 15. Dunphy CM, Gouhier TC, Chu ND, & Vollmer SV (2019) Structure and stability of the  
875 coral microbiome in space and time. *Sci Rep-UK* 9(1):1-13.
- 876 16. Chu ND & Vollmer SV (2016) Caribbean corals house shared and host-specific microbial  
877 symbionts over time and space. *Env Microbiol Rep* 8(4):493-500.
- 878 17. Hester ER, Barott KL, Nulton J, Vermeij MJ, & Rohwer FL (2016) Stable and sporadic  
879 symbiotic communities of coral and algal holobionts. *The ISME journal* 10(5):1157-1169.

880 18. Huggett MJ & Apprill A (2019) Coral microbiome database: Integration of sequences  
881 reveals high diversity and relatedness of coral-associated microbes. *Env Microbiol Rep*  
882 11(3):372-385.

883 19. Pollock FJ, *et al.* (2018) Coral-associated bacteria demonstrate phylosymbiosis and  
884 cophylogeny. *Nat Commun* 9(1):1-13.

885 20. Zaneveld JR, *et al.* (2016) Overfishing and nutrient pollution interact with temperature to  
886 disrupt coral reefs down to microbial scales. *Nat Commun* 7(1):1-12.

887 21. Mayer B, Rixen T, & Pohlmann T (2018) The spatial and temporal variability of air-sea  
888 CO<sub>2</sub> fluxes and the effect of net coral reef calcification in the Indonesian Seas: A  
889 numerical sensitivity study. *Frontiers in Marine Science* 5:116.

890 22. Morrow K, Muller E, & Lesser M (2018) How does the coral microbiome cause, respond  
891 to, or modulate the bleaching process? *Coral bleaching*, (Springer), pp 153-188.

892 23. Thornhill DJ, LaJeunesse TC, Kemp DW, Fitt WK, & Schmidt GW (2006) Multi-year,  
893 seasonal genotypic surveys of coral-algal symbioses reveal prevalent stability or post-  
894 bleaching reversion. *Marine Biology* 148(4):711-722.

895 24. Toller WW, Rowan R, & Knowlton N (2001) Repopulation of zooxanthellae in the  
896 Caribbean corals Montastraea annularis and M. faveolata following experimental and  
897 disease-associated bleaching. *The Biological Bulletin* 201(3):360-373.

898 25. Jones RJ & Yellowlees D (1997) Regulation and control of intracellular algae (=  
899 zooxanthellae) in hard corals. *Philosophical Transactions of the Royal Society of*  
900 *London. Series B: Biological Sciences* 352(1352):457-468.

901 26. Szmant A & Gassman N (1990) The effects of prolonged "bleaching" on the tissue  
902 biomass and reproduction of the reef coral Montastrea annularis. *Coral reefs* 8(4):217-  
903 224.

904 27. Jokiel PL & Coles S (1977) Effects of temperature on the mortality and growth of  
905 Hawaiian reef corals. *Marine Biology* 43(3):201-208.

906 28. Grottoli AG, *et al.* (2014) The cumulative impact of annual coral bleaching can turn some  
907 coral species winners into losers. *Global Change Biol* 20(12):3823-3833.

908 29. Berkelmans R & Van Oppen MJ (2006) The role of zooxanthellae in the thermal  
909 tolerance of corals: a 'nugget of hope' for coral reefs in an era of climate change.  
910 *Proceedings of the Royal Society B: Biological Sciences* 273(1599):2305-2312.

911 30. Silverstein RN, Cunning R, & Baker AC (2015) Change in algal symbiont communities  
912 after bleaching, not prior heat exposure, increases heat tolerance of reef corals. *Global*  
913 *Change Biol* 21(1):236-249.

914 31. Baker AC (2004) Symbiont diversity on coral reefs and its relationship to bleaching  
915 resistance and resilience. *Coral health and disease*, (Springer), pp 177-194.

916 32. Abrego D, Ulstrup KE, Willis BL, & van Oppen MJ (2008) Species-specific interactions  
917 between algal endosymbionts and coral hosts define their bleaching response to heat  
918 and light stress. *Proceedings of the Royal Society B: Biological Sciences*  
919 275(1648):2273-2282.

920 33. Baird AH, Bhagooli R, Ralph PJ, & Takahashi S (2009) Coral bleaching: the role of the  
921 host. *Trends Ecol Evol* 24(1):16-20.

922 34. Henley EM, *et al.* (2022) Growth and survival among Hawaiian corals outplanted from  
923 tanks to an ocean nursery are driven by individual genotype and species differences  
924 rather than preconditioning to thermal stress. *PeerJ* 10:e13112.

925 35. Drury C (2020) Resilience in reef-building corals: The ecological and evolutionary  
926 importance of the host response to thermal stress. *Mol Ecol* 29(3):448-465.

927 36. Barshis DJ, *et al.* (2013) Genomic basis for coral resilience to climate change. *Proc Natl*  
928 *Acad Sci U S A* 110(4):1387-1392.

929 37. Bay RA & Palumbi SR (2014) Multilocus adaptation associated with heat resistance in  
930 reef-building corals. *Curr Biol* 24(24):2952-2956.

931 38. Weis VM (2010) The susceptibility and resilience of corals to thermal stress: adaptation,  
932 acclimatization or both? *Mol Ecol* 19(8):1515-1517.

933 39. Pootakham W, et al. (2019) Heat-induced shift in coral microbiome reveals several  
934 members of the Rhodobacteraceae family as indicator species for thermal stress in  
935 *Porites lutea*. *Microbiologyopen* 8(12):e935.

936 40. Ziegler M, Seneca FO, Yum LK, Palumbi SR, & Voolstra CR (2017) Bacterial community  
937 dynamics are linked to patterns of coral heat tolerance. *Nat Commun* 8:14213.

938 41. Petrou K, Nunn BL, Padula MP, Miller DJ, & Nielsen DA (2021) Broad scale proteomic  
939 analysis of heat-destabilised symbiosis in the hard coral *Acropora millepora*. *Sci Rep*  
940 11(1):19061.

941 42. Morris LA, Voolstra CR, Quigley KM, Bourne DG, & Bay LK (2019) Nutrient availability  
942 and metabolism affect the stability of coral–Symbiodiniaceae symbioses. *Trends  
943 Microbiol* 27(8):678-689.

944 43. Hughes TP, et al. (2018) Global warming transforms coral reef assemblages. *Nature*  
945 556(7702):492-496.

946 44. Coles SL, Jokiel PL, & Lewis CR (1976) Thermal tolerance in tropical versus subtropical  
947 Pacific reef corals.

948 45. Jokiel PL & Brown EK (2004) Global warming, regional trends and inshore  
949 environmental conditions influence coral bleaching in Hawaii. *Global Change Biol*  
950 10(10):1627-1641.

951 46. Hoeke RK, Jokiel PL, Buddemeier RW, & Brainard RE (2011) Projected changes to  
952 growth and mortality of Hawaiian corals over the next 100 years. *PLoS one* 6(3):e18038.

953 47. Gibbin EM, Putnam HM, Gates RD, Nitschke MR, & Davy SK (2015) Species-specific  
954 differences in thermal tolerance may define susceptibility to intracellular acidosis in reef  
955 corals. *Marine Biology* 162(3):717-723.

956 48. Riffle M, et al. (2017) MetaGOMics: A Web-Based Tool for Peptide-Centric Functional  
957 and Taxonomic Analysis of Metaproteomics Data. *Proteomes* 6(1).

958 49. Botos I & Wlodawer A (2003) Cyanovirin-N: a sugar-binding antiviral protein with a new  
959 twist. *Cellular and Molecular Life Sciences CMLS* 60(2):277-287.

960 50. Rodrigues LJ & Grottoli AG (2007) Energy reserves and metabolism as indicators of  
961 coral recovery from bleaching. *Limnol Oceanogr Lett* 52(5):1874-1882.

962 51. Mallick H, et al. (2021) Multivariable association discovery in population-scale meta-  
963 omics studies. *PLoS Comput Biol* 17(11):e1009442.

964 52. Ricci C, et al. (2019) Proteomic Characterization of Immune Responses and Post-  
965 infection Dynamics of *Eunicea calyculata* to late stage *Eunicea* Black Disease.  
966 *INTEGRATIVE AND COMPARATIVE BIOLOGY*, (OXFORD UNIV PRESS INC  
967 JOURNALS DEPT, 2001 EVANS RD, CARY, NC 27513 USA), pp E192-E192.

968 53. Stuhr M, et al. (2018) Disentangling thermal stress responses in a reef-calcifier and its  
969 photosymbionts by shotgun proteomics. *Sci Rep* 8(1):3524.

970 54. Weston AJ, et al. (2015) Proteomics Links the Redox State to Calcium Signaling During  
971 Bleaching of the Scleractinian Coral *Acropora microphthalma* on Exposure to High Solar  
972 Irradiance and Thermal Stress [S]. *Molecular & Cellular Proteomics* 14(3):585-595.

973 55. Petrou K, Nunn B, Padula M, Miller D, & Nielsen D (2021) Broad scale proteomic  
974 analysis of heat-destabilised symbiosis in the hard coral *Acropora millepora*. *Sci Rep-Uk*  
975 11(1):1-16.

976 56. Axworthy JB, et al. (2022) Shotgun Proteomics Identifies Active Metabolic Pathways in  
977 Bleached Coral Tissue and Intraskeletal Compartments. *Frontiers in Marine Science*  
978 9:50.

979 57. Tisthammer KH, Timmins-Schiffman E, Seneca FO, Nunn BL, & Richmond RH (2021)  
980 Physiological and molecular responses of lobe coral indicate nearshore adaptations to  
981 anthropogenic stressors. *Sci Rep-Uk* 11(1):1-11.

982 58. Nunn BL, *et al.* (2013) Diatom proteomics reveals unique acclimation strategies to  
983 mitigate Fe limitation. *PLoS One* 8(10):e75653.

984 59. Aertsen A & Michiels CW (2005) Diversify or die: generation of diversity in response to  
985 stress. *Critical reviews in microbiology* 31(2):69-78.

986 60. Yan S-P, Zhang Q-Y, Tang Z-C, Su W-A, & Sun W-N (2006) Comparative proteomic  
987 analysis provides new insights into chilling stress responses in rice. *Molecular & cellular*  
988 *proteomics* 5(3):484-496.

989 61. Palardy JE, Rodrigues LJ, & Grottoli AG (2008) The importance of zooplankton to the  
990 daily metabolic carbon requirements of healthy and bleached corals at two depths.  
991 *Journal of experimental marine biology and ecology* 367(2):180-188.

992 62. Lawe DC, Patki V, Heller-Harrison R, Lambright D, & Corvera S (2000) The FYVE  
993 domain of early endosome antigen 1 is required for both phosphatidylinositol 3-  
994 phosphate and Rab5 binding: critical role of this dual interaction for endosomal  
995 localization. *Journal of Biological Chemistry* 275(5):3699-3705.

996 63. Mohamed AR, *et al.* (2018) Deciphering the nature of the coral–Chromera association.  
997 *The ISME journal* 12(3):776-790.

998 64. Koul A, Herget T, Klebl B, & Ullrich A (2004) Interplay between mycobacteria and host  
999 signalling pathways. *Nature reviews. Microbiology* 2(3):189-202.

1000 65. Grottoli AG, Rodrigues LJ, & Palardy JE (2006) Heterotrophic plasticity and resilience in  
1001 bleached corals. *Nature* 440(7088):1186-1189.

1002 66. Swart PK (1983) Carbon and oxygen isotope fractionation in scleractinian corals: a  
1003 review. *Earth-science reviews* 19(1):51-80.

1004 67. Yano T, Yoshida N, Yu F, Wakamatsu M, & Takagi H (2015) The glyoxylate shunt is  
1005 essential for CO<sub>2</sub>-requiring oligotrophic growth of *Rhodococcus erythropolis* N9T-4.  
1006 *Applied microbiology and biotechnology* 99(13):5627-5637.

1007 68. Voolstra CR, *et al.* (2021) Contrasting heat stress response patterns of coral holobionts  
1008 across the Red Sea suggest distinct mechanisms of thermal tolerance. *Mol Ecol*  
1009 30(18):4466-4480.

1010 69. Percudani R, Montanini B, & Ottonello S (2005) The anti-HIV cyanovirin-N domain is  
1011 evolutionarily conserved and occurs as a protein module in eukaryotes. *Proteins: Structure,*  
1012 *Function, and Bioinformatics* 60(4):670-678.

1013 70. Gardner SG, *et al.* (2019) Coral microbiome diversity reflects mass coral bleaching  
1014 susceptibility during the 2016 El Niño heat wave. *Ecology and evolution* 9(3):938-956.

1015 71. Ziegler M, *et al.* (2019) Coral bacterial community structure responds to environmental  
1016 change in a host-specific manner. *Nat Commun* 10(1):3092.

1017 72. Stalder T, Press MO, Sullivan S, Liachko I, & Top EM (2019) Linking the resistome and  
1018 plasmidome to the microbiome. *The ISME journal* 13(10):2437-2446.

1019 73. Kellogg CA (2019) Microbiomes of stony and soft deep-sea corals share rare core  
1020 bacteria. *Microbiome* 7(1):1-13.

1021 74. Mashini AG, *et al.* (2023) The Influence of Symbiosis on the Proteome of the Exaiptasia  
1022 Endosymbiont *Breviolum minutum*. *Microorganisms* 11(2):292.

1023 75. Pernice M, *et al.* (2012) A single-cell view of ammonium assimilation in coral–  
1024 dinoflagellate symbiosis. *The ISME journal* 6(7):1314-1324.

1025 76. Roberts JM, Fixter L, & Davies P (2001) Ammonium metabolism in the symbiotic sea  
1026 anemone *Anemonia viridis*. *Hydrobiologia* 461:25-35.

1027 77. Biscéré T, *et al.* (2018) Enhancement of coral calcification via the interplay of nickel and  
1028 urease. *Aquatic Toxicology* 200:247-256.

1029 78. Grover R, Maguer J-F, Allemand D, & Ferrier-Pagès C (2006) Urea uptake by the  
1030 scleractinian coral *Stylophora pistillata*. *Journal of Experimental Marine Biology and*  
1031 *Ecology* 332(2):216-225.

1032 79. Barnes D & Crossland C (1976) Urease activity in the staghorn coral, *Acropora*  
1033 acuminata. *Comparative Biochemistry and Physiology Part B: Comparative Biochemistry*  
1034 55(3):371-376.

1035 80. Chen M-C, et al. (2005) ApRab11, a cnidarian homologue of the recycling regulatory  
1036 protein Rab11, is involved in the establishment and maintenance of the Aiptasia–  
1037 *Symbiodinium* endosymbiosis. *Biochemical and biophysical research communications*  
1038 338(3):1607-1616.

1039 81. Downs CA, et al. (2009) Symbiophagy as a cellular mechanism for coral bleaching.  
1040 *Autophagy* 5(2):211-216.

1041 82. Araki N (2006) Role of microtubules and myosins in Fc gamma receptor-mediated  
1042 phagocytosis. *Front Biosci* 11(2):1479-1490.

1043 83. Kvennafors ECE, Leggat W, Hoegh-Guldberg O, Degnan BM, & Barnes AC (2008) An  
1044 ancient and variable mannose-binding lectin from the coral *Acropora millepora* binds  
1045 both pathogens and symbionts. *Developmental & Comparative Immunology*  
1046 32(12):1582-1592.

1047 84. Fujita T, Matsushita M, & Endo Y (2004) The lectin-complement pathway—its role in  
1048 innate immunity and evolution. *Immunological reviews* 198(1):185-202.

1049 85. Moncada DM, Kammanadiminti SJ, & Chadee K (2003) Mucin and Toll-like receptors in  
1050 host defense against intestinal parasites. *Trends in parasitology* 19(7):305-311.

1051 86. Rivera H & Davies S (2021) Symbiosis maintenance in the facultative coral, *Oculina*  
1052 *arbuscula*, relies on nitrogen cycling, cell cycle modulation, and immunity. *Sci Rep-Uk*  
1053 11(1):21226.

1054 87. Mydlarz LD, McGinty ES, & Harvell CD (2010) What are the physiological and  
1055 immunological responses of coral to climate warming and disease? *J Exp Biol*  
1056 213(6):934-945.

1057 88. Bin P, Huang R, & Zhou X (2017) Oxidation resistance of the sulfur amino acids:  
1058 methionine and cysteine. *BioMed research international* 2017.

1059 89. Ruiz-Jones LJ & Palumbi SR (2017) Tidal heat pulses on a reef trigger a fine-tuned  
1060 transcriptional response in corals to maintain homeostasis. *Science advances*  
1061 3(3):e1601298.

1062 90. Sundborger AC & Hinshaw JE (2014) Regulating dynamin dynamics during endocytosis.  
1063 *F1000prime reports* 6.

1064 91. Lehninger AL, Nelson DL, Cox MM, & Cox MM (2005) *Lehninger principles of*  
1065 *biochemistry* (Macmillan).

1066 92. Lindqvist Y, Schneider G, Ermler U, & Sundström M (1992) Three-dimensional structure  
1067 of transketolase, a thiamine diphosphate dependent enzyme, at 2.5 Å resolution. *The*  
1068 *EMBO journal* 11(7):2373-2379.

1069 93. Schnuck JK, Sunderland KL, Kuennen MR, & Vaughan RA (2016) Characterization of  
1070 the metabolic effect of  $\beta$ -alanine on markers of oxidative metabolism and mitochondrial  
1071 biogenesis in skeletal muscle. *Journal of Exercise Nutrition & Biochemistry* 20(2):34.

1072 94. Hillyer KE, Tumanov S, Villas-Bôas S, & Davy SK (2016) Metabolite profiling of symbiont  
1073 and host during thermal stress and bleaching in a model cnidarian–dinoflagellate  
1074 symbiosis. *J Exp Biol* 219(4):516-527.

1075 95. Hambleton EA, et al. (2019) Sterol transfer by atypical cholesterol-binding NPC2  
1076 proteins in coral-algal symbiosis. *Elife* 8:e43923.

1077 96. Tortorelli G, et al. (2022) Cell surface carbohydrates of symbiotic dinoflagellates and  
1078 their role in the establishment of cnidarian–dinoflagellate symbiosis. *The ISME journal*  
1079 16(1):190-199.

1080 97. Kopp C, et al. (2015) Subcellular investigation of photosynthesis-driven carbon  
1081 assimilation in the symbiotic reef coral *Pocillopora damicornis*. *Mbio* 6(1):e02299-02214.

1082 98. Ngugi DK, Ziegler M, Duarte CM, & Voolstra CR (2020) Genomic blueprint of glycine  
1083 betaine metabolism in coral metaorganisms and their contribution to reef nitrogen  
1084 budgets. *Isaacse* 23(5):101120.

1085 99. O'Brien PA, et al. (2020) Diverse coral reef invertebrates exhibit patterns of  
1086 phyllosymbiosis. *The ISME journal* 14(9):2211-2222.

1087 100. Palmer C & Traylor-Knowles N (2012) Towards an integrated network of coral immune  
1088 mechanisms. *Proceedings of the Royal Society B: Biological Sciences* 279(1745):4106-  
1089 4114.

1090 101. Matthews JL, et al. (2017) Optimal nutrient exchange and immune responses operate in  
1091 partner specificity in the cnidarian-dinoflagellate symbiosis. *Proceedings of the National  
1092 Academy of Sciences* 114(50):13194-13199.

1093 102. Thurber RV, et al. (2009) Metagenomic analysis of stressed coral holobionts.  
1094 *Environmental microbiology* 11(8):2148-2163.

1095 103. Harvell D, et al. (2007) Coral disease, environmental drivers, and the balance between  
1096 coral and microbial associates. *Oceanography* 20:172-195.

1097 104. Vega Thurber RL, et al. (2014) Chronic nutrient enrichment increases prevalence and  
1098 severity of coral disease and bleaching. *Global Change Biol* 20(2):544-554.

1099 105. Frazier M, Helmkampf M, Bellinger MR, Geib SM, & Takabayashi M (2017) De novo  
1100 metatranscriptome assembly and coral gene expression profile of Montipora capitata  
1101 with growth anomaly. *BMC genomics* 18:1-11.

1102 106. Choi H, Kim S, Fermin D, Tsou CC, & Nesvizhskii AI (2015) QPROT: Statistical method  
1103 for testing differential expression using protein-level intensity data in label-free  
1104 quantitative proteomics. *J Proteomics* 129:121-126.

1105 107. Bolyen E, et al. (2019) Reproducible, interactive, scalable and extensible microbiome  
1106 data science using QIIME 2. *Nat Biotechnol* 37(8):852-857.

1107 108. Anderson MJ (2001) A new method for non-parametric multivariate analysis of variance.  
1108 *Austral ecology* 26(1):32-46.

1109

**Figure 1**

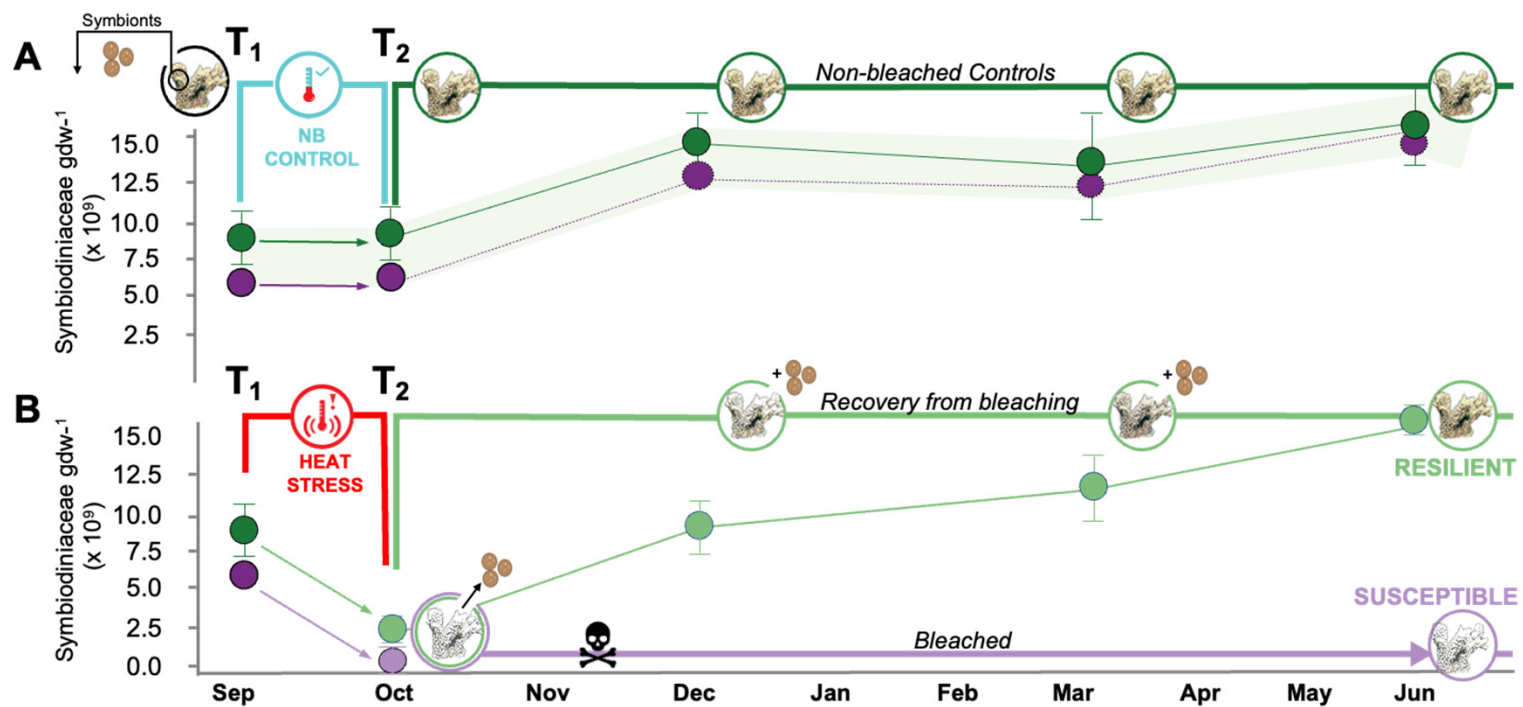


**Figure 2** bioRxiv preprint doi: <https://doi.org/10.1101/2024.04.02.587798>; this version posted April 3, 2024. The copyright holder for this preprint (which was not certified by peer review) is the author/funder, who has granted bioRxiv a license to display the preprint in perpetuity. It is made available under aCC-BY-NC-ND 4.0 International license.

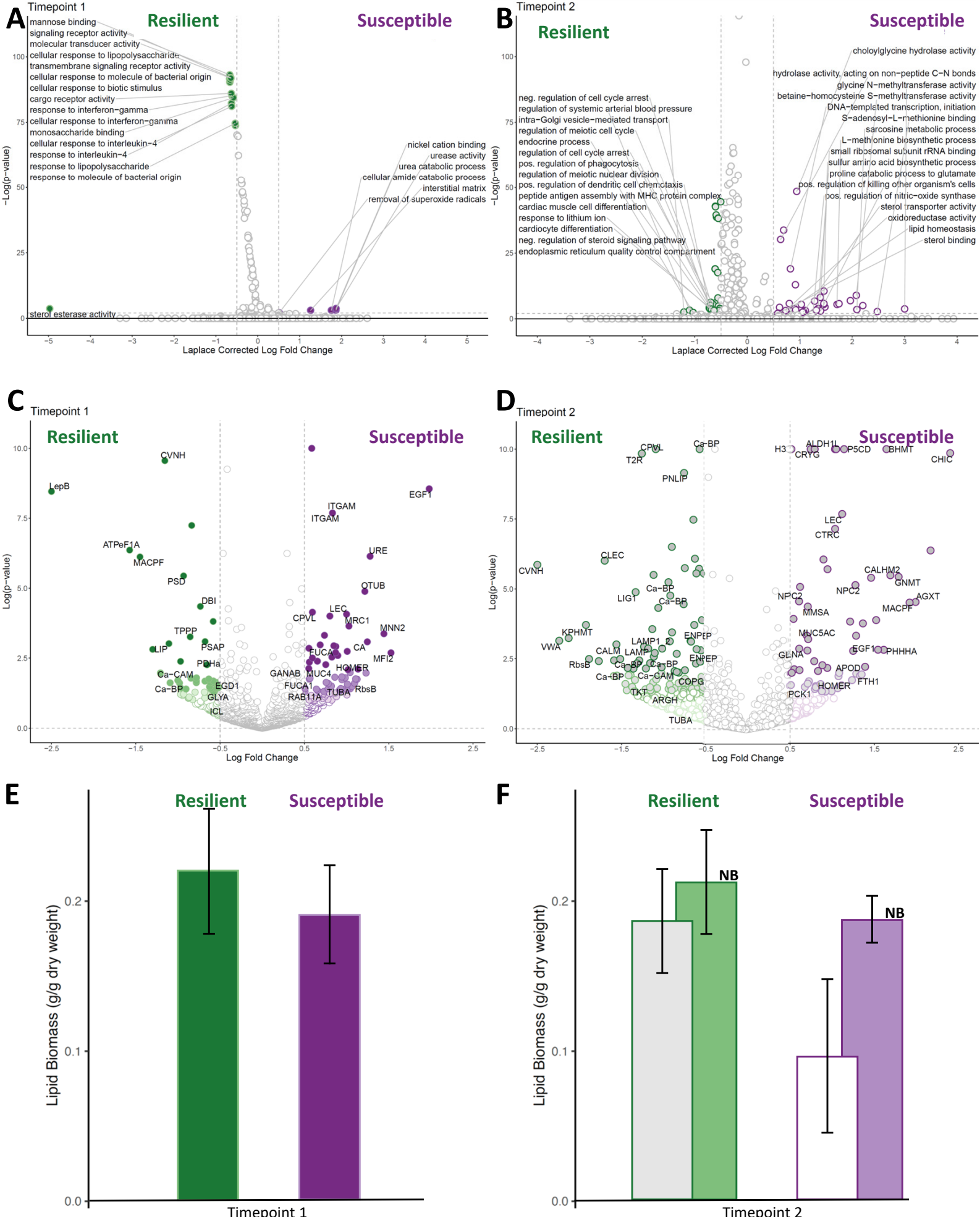


# Figure 3



**Figure 4**

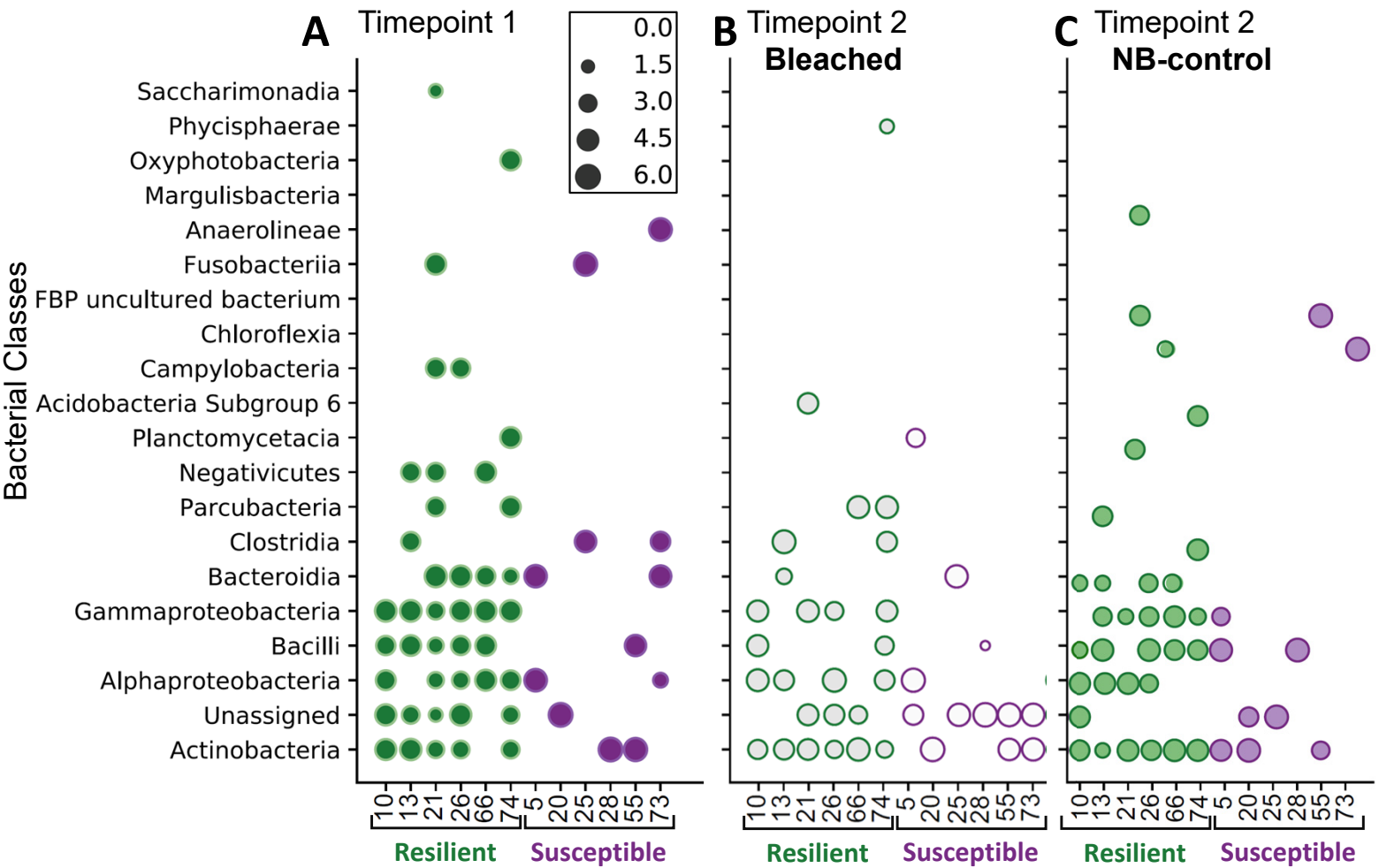


## Figure 5

